Geological Survey of Finland

Bulletin 392

Comparison of petrophysical and rock geochemical data in the Tampere–Hämeenlinna area, southern Finland

by Raimo Lahtinen and Juha V. Korhonen

Geological Survey of Finland
Espoo 1996

Lahtinen, R. and Korhonen, J., 1996. Comparison of petrophysical and rock geochemical data in the Tampere-Hämeenlinna area, southern Finland. Geological Survey of Finland, Bulletin 392, 45 p.

Geol. Surv. Finland, Bull. 392

Errata

	printed	should be
p, 27, Fig. 16, text line 7:	m^3/kg	10^{-8} m^3/kg
p, 27, Fig. 16, text line 8:	m^3/kg	10^{-8} m^3/kg
p. 28, right col., line 4:	m^3/kg	10^{-8} m^3/kg
p. 28, right col., line 6:	m^3/kg	10^{-8} m^3/kg

Geological Survey of Finland, Bulletin 392

COMPARISON OF PETROPHYSICAL AND ROCK GEOCHEMICAL DATA IN THE TAMPERE–HÄMEENLINNA AREA, SOUTHERN FINLAND

by

RAIMO LAHTINEN AND JUHA V. KORHONEN

with 20 figures, 4 tables

GEOLOGICAL SURVEY OF FINLAND
ESPOO 1996

Lahtinen, Raimo & Korhonen, Juha V. 1996. Comparison of petrophysical and rock geochemical data in the Tampere–Hämeenlinna area, southern Finland. *Geological Survey of Finland, Bulletin 392.* 45 pages, 20 figures, 4 tables.

Mass susceptibilities and Q-ratios were calculated from bulk densities, volume susceptibilities and intensities of NRM measured in 403 bedrock samples. These values were then compared with paramagnetic susceptibilities (k_{pc}) from the chemical data calculated by Curie's law, and with estimated ferrimagnetic susceptibilities (k_{fc}) and ferrimagnetic Q-ratios (Q_{fc}). Since even the most paramagnetic samples show a small ferrimagnetic component (average $2 \cdot 10^{-8} m^3/kg$), pure paramagnetic samples are either rare or absent.

The correlation of bulk density with FeO+MnO+MgO is good in volcanic and plutonic rocks and poorer in sedimentary rocks. The sedimentary rocks belong mainly to the paramagnetic population and the higher susceptibilities are normally due to the occurrence of pyrrhotite. Subduction-related volcanic rocks tend to be magnetite-bearing, but many of the samples are brecciated and/or pyroclastic rocks and the relationship is not clear-cut. Most of the calc-alkaline (I-type) syn-tectonic granitoids (1.89–1.88 Ga) are paramagnetic, while magnetite occurs in rocks with a comingled and hybrid nature. Most of the late- to post-tectonic (I-type) granites in the northern part show ferrimagnetic characteristics, and granitoids from the central sedimentary part and the late S-type granites show paramagnetic characteristics.

The magnetization in the northern and southern volcano-plutonic complexes of the study area is mainly due to magnetite and these areas differ from the central sediment-dominated area, which overall exhibits a reducing environment and pyrrhotite predominance. The magnetic low (common base level -250 nT of DGRF-65 total field anomaly) in the central collision zone, in contrast with the high deep magnetic anomaly components in the south (+80 nT) and north (+100 nT), indicates a great thickness for the sedimentary pile in the collision zone. Both southern and northern parts are underlain by a deep magnetic source, and the southernmost part is also underlain by mafic rocks and/or sedimentary restites related to the 1.84–1.81 Ga granites.

Key words (GeoRef Thesaurus, AGI): petrophysics, metavolcanic rocks, metasedimentary rocks, plutonic rocks, bulk density, magnetic properties, magnetic anomalies, Bouguer anomaly, geochemistry, upper crust, Proterozoic, Tampere, Hämeenlinna, Finland

Raimo Lahtinen & Juha V. Korhonen, Geological Survey of Finland,
P. O. Box 96, FIN-02151 ESPOO, FINLAND

E-mail: raimo.lahtinen@gsf.fi
juha.korhonen@gsf.fi

ISBN 951-690-668-0
ISSN 0367-522X

Vammalan Kirjapaino Oy 1997

CONTENTS

PREFACE

The bedrock of Finland, which is mainly Precambrian in age, is on average covered by some 7 metres of Quaternary sediments, such that only 3 % of the surface area is exposured. Because till, the most abundant material in the overburden, was derived from bedrock it generally corresponds compositionally to bedrock, though because of mixing and transport, till analysis only provides an overall view. On the other hand, the degree of exposure makes representative sampling of bedrock a real challenge.

A rock geochemistry research program was established in 1991 by the geochemistry department of Geological Survey of Finland. The final decision to start the research program was preceded by intensive discussions on the need, on the content, and on the methods of the program throughout most of the whole 1980's. Essential support to the program was given by Prof. G. Govett in his reports in 1986 and 1988, when he was evaluating the scientific achievements and role of the geochemistry department. The rock geochemistry program started and took shape rapidly following his second evaluation report. Raimo Lahtinen made the first preliminary project proposal in 1988, and a working group consisting of Pekka Lestinen (chairman), R. Lahtinen and Esko Korkiakoski was established in the department in order to prepare a plan for the whole research program. Their proposal was finalized already by the end of 1988. The essential content of this proposal was a pilot study project for the years 1989–1990. Because this kind of research program was quite unique even from an international viewpoint, it was natural to commence with a pilot study more thorough than usual. These publications were collected from the results of the pilot study, processing the data, and their practical applications. The research program began very soon after the results of pilot study were available, and the field work phase of the research program has already been completed.

The main emphasis of the pilot phase was to study the representativeness of sampling, selecting the correct sampling grid, determining the amount of samples needed, and selecting the analytical methods. All these more or less technical aspects were reported in an internal report in 1991.

One of the main principles of the rock geochemistry research program has been the use of the most modern analytical techniques, which make possible, in addition to ordinary major element analysis the obtaining of high quality data for minor and trace elements. In addition to geochemical data, petrophysical parameters of the samples are determined. The public domain data bank covering the whole country, which will be available on completion of the program, thus offers an exceptionally broad and high quality source of data for application and interpretation in bedrock geochemistry studies.

The aim of the rock research program was determined 'to collect geochemical data concentrated in trace elements from the area of the whole country, to produce background data for interpretations of regional till geochemistry data, to classify the rock types, and to clarify the metallogeny of the bedrock.

Geochemical changes pertaining to the crustal evolution will be studied, too'.

These issues of the GSF Bulletin are concerned with application of the data and provide examples of potential ways of using the data. Recently it has also been realized that the data are valuable in other quite unforeseen applications, such as in evaluation of water quality in drilled wells. The final results of the research program are planned to be published as soon as possible for the benefit not only of researchers in Finland but also in other countries interested in problems of Archaean and Proterozoic bedrock as well as for those studing regional health and environmental problems.

Espoo 19.11.1996 *Reijo Salminen*

Publications:

Lahtinen, R. 1996. Geochemistry of Palaeoproterozoic supracrustal and plutonic rocks in the Tampere–Hämeenlinna area, southern Finland. Geological Survey of Finland, Bulletin 389. 113 p.

Lahtinen, R. & Lestinen, P. 1996. Background variation of ore-related elements and regional-scale mineralization indications in Palaeoproterozoic bedrock in the Tampere–Hämeenlinna area, southern Finland. Geological Survey of Finland, Bulletin 390. 38 p.

Lestinen, P., Savolainen, H. & Lahtinen, R. 1996. New methods applying bedrock lithological and geochemical data to the interpretation of regional till geochemical data: a study in the Tampere–Hämeenlinna area, southern Finland. Geological Survey of Finland, Bulletin 391. 37 p.

Lahtinen, R. & Korhonen, J.V. 1996. Comparison of petrophysical and rock geochemical data in the Tampere–Hämeenlinna area, southern Finland. Geological Survey of Finland, Bulletin 392. 45 p.

Sandström, H. 1996. The analytical methods and the precision of the element determinations used in the regional bedrock geochemistry in the Tampere–Hämeenlinna area, southern Finland. Geological Survey of Finland, Bulletin 393. 25 p.

INTRODUCTION

The Geological Survey of Finland (GSF) has been carrying out airborne geophysical surveys since 1951. The high-altitude survey of the whole country carried out at a flying height of 150 m and with a track separation of 400 m was completed in 1972. The low-altitude programme, with a flying height of 30–40 m and track separation of 200 m, was begun in the same year. The coverage of the latter is now over 75% of the Finnish mainland. The airborne geophysical programmes are intended to support mineral exploration and geological mapping. Because most of the Finnish bedrock is covered by overburden, aeromagnetic information is essential to draw conclusions about the extent of geological formations and to interpret the structural and metamorphic history. The magnetic properties of the rocks have been measured since the 1950s to facilitate interpretation of the maps, and the data are stored in a petrophysical register at the GSF (Puranen et al. 1978). A petrophysical mapping programme covering the whole of Finland with density and magnetic measurements of rock samples was carried out between 1980 and 1992 (Korhonen et al. 1993). The petrophysical data are used to assign physical properties to source bodies, to correlate rock types and formations and to assist genetic interpretations.

The Tampere–Hämeenlinna study area lies entirely within the Palaeoproterozoic Svecofennian domain of central Finland and is geophysically characterized by a regional magnetic low (minimum, -250 nT of DGRF-65 total field anomaly) in the middle, bordered by regional highs to the north (maximum, 350 nT) and south (maximum, 400 nT). Averaging was done in 20x20 km cells. The central part, especially its southern and northern ends, exhibits good electrical conductance (>1 S), whereas the southern and northern parts of the area do not (Fig. 1a). The maximum Bouguer anomalies are +2 mGal, -12 mGal and -22 mGal for the southern, central and northern parts respectively. The central part is distinguished from the northern and southern parts by sharp gravity lows (Fig. 1b).

Two volcanic-bearing schist belts cut through the area: the Tampere Schist Belt (TSB) in the north and the Hämeenlinna Schist Belt (HSB) in the south (Fig. 2a). The TSB changes to a granitoid-dominated area in the north (NTSB), which is the southern part of the Central Finland Granitoid Complex (CFGC). In the eastern part of the NTSB lies the small Hirsilä Schist Belt (HiSB). The NTSB coincides with the regional magnetic high in the north. Between the TSB and HSB lies the Mica gneiss–migmatite Belt (MB), coinciding with the regional magnetic low and conducting area. The HSB exhibits locally strong aeromagnetic anomalies. The southernmost part of the Microcline granite Complex (MC), which contains migmatitic supracrustal rocks, coincides with a regional aeromagnetic maximum. More detailed descriptions of the geology and geochemistry of the study area with interpretations for the origin of rocks and crustal evolution of the area can be found in Lahtinen (1996).

In this study, we compare the geochemical and petrophysical data of 403 bedrock samples (set A) as a means of correlating the mineralogy and chemical composition with the petrophysical properties of rocks. Lahtinen's clas-

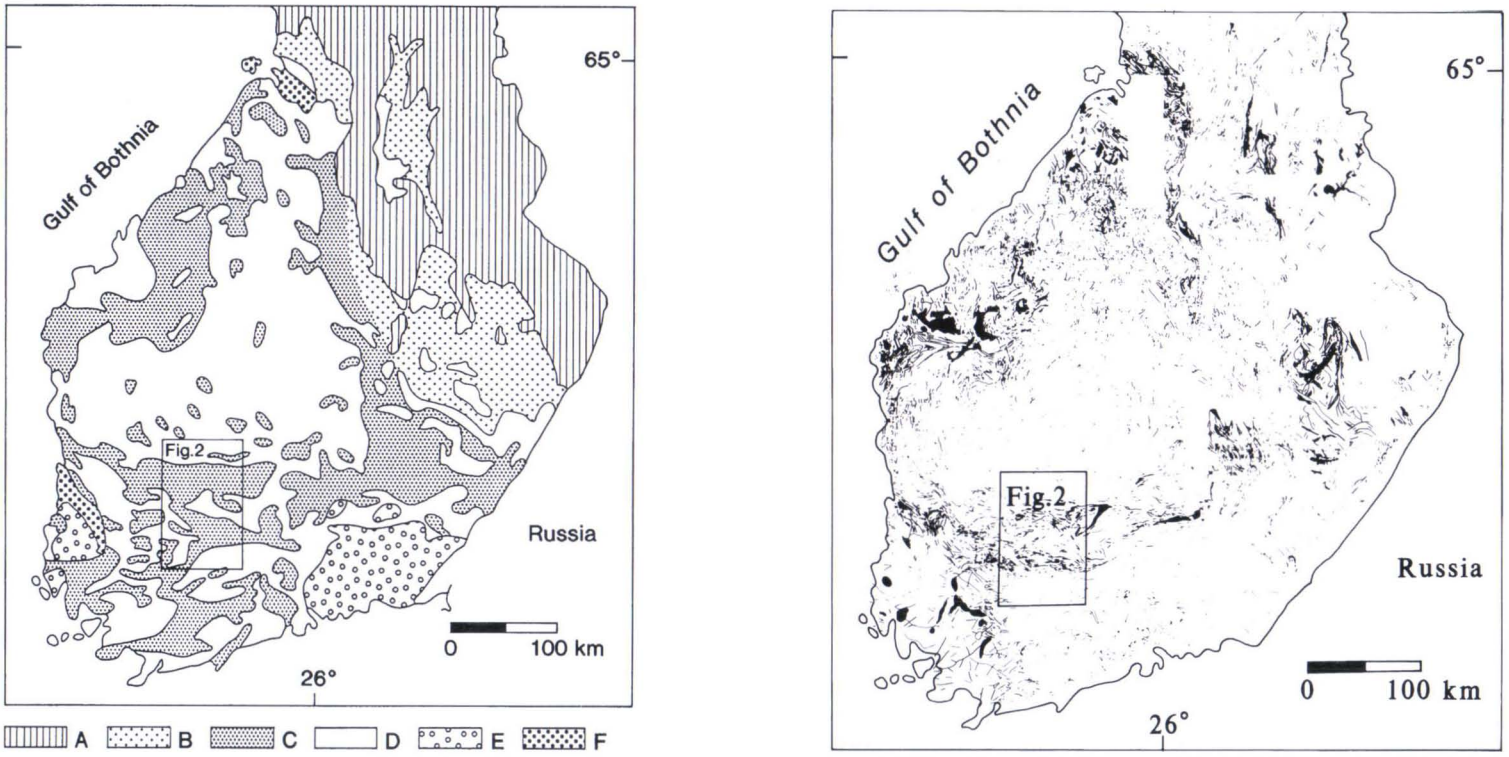

Fig. 1a. The geological (left) and electrical conductance (right, Fig. 29a in Peltoniemi 1992) maps of southern Finland. Simplified geological map of southern Finland after Simonen (1980). A. Archaean rocks; B. Karelian schists; C. Svecofennian schists, gneisses and migmatites; D. Svecofennian plutonic rocks; E. rapakivi granites; F. Jotnian sedimentary rocks. Electrical conductance: black lines and area (>0.5 S). The study area (see Fig. 2) is shown in outline.

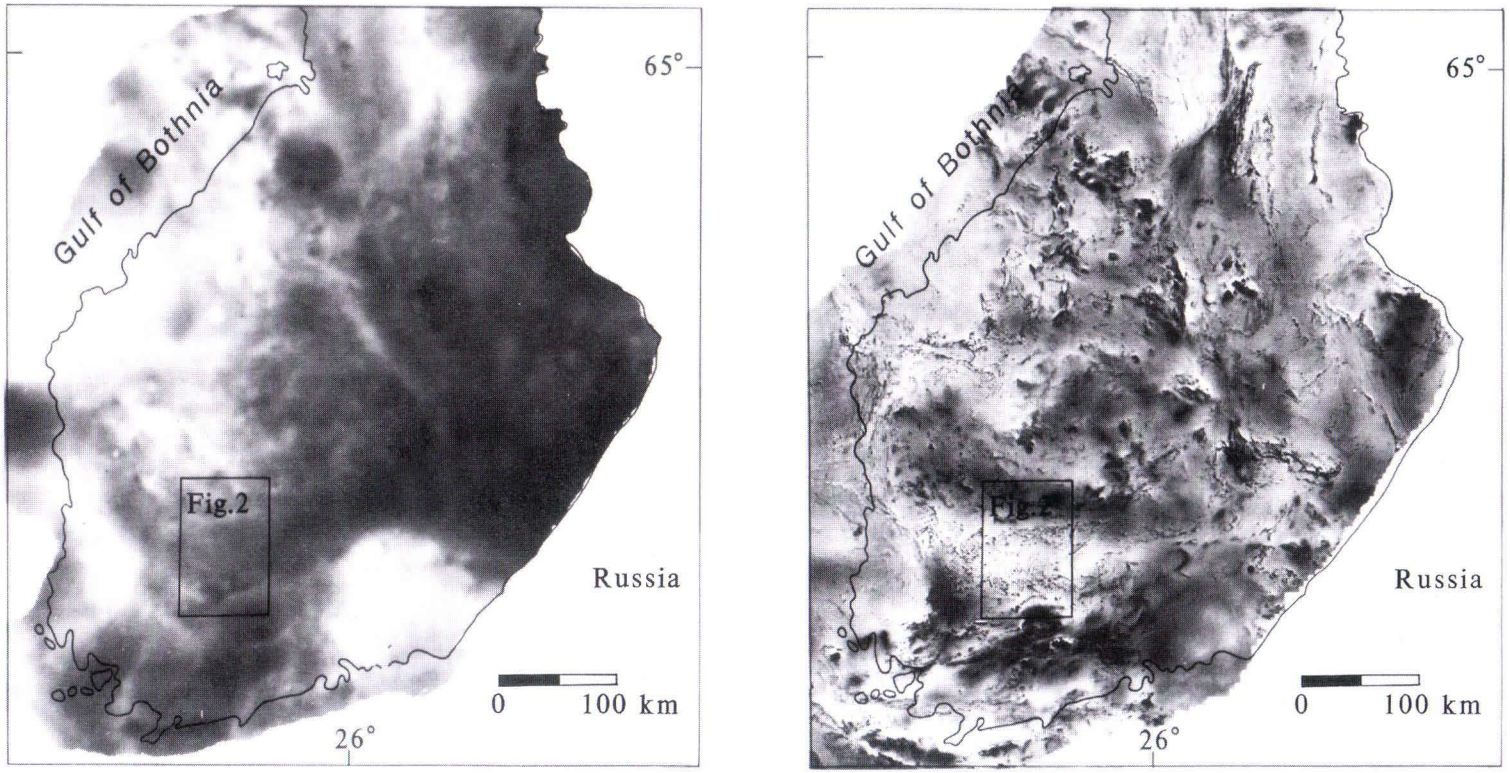

Fig 1b. Bouguer anomaly (left, interpolated by S. Elo based on data of the Finnish Geodetic Institute) and high-altitude (150 m) aeromagnetic DGRF-65 anomaly (right, Fig. 28a in Korhonen 1992) maps of southern Finland. Grey tones (Bouguer gravity): dark +16 mGal, light -48 mGal. Grey tones (aeromagnetic): dark +600 nT, light -600 nT. The study area (see Fig. 2) is shown in outline.

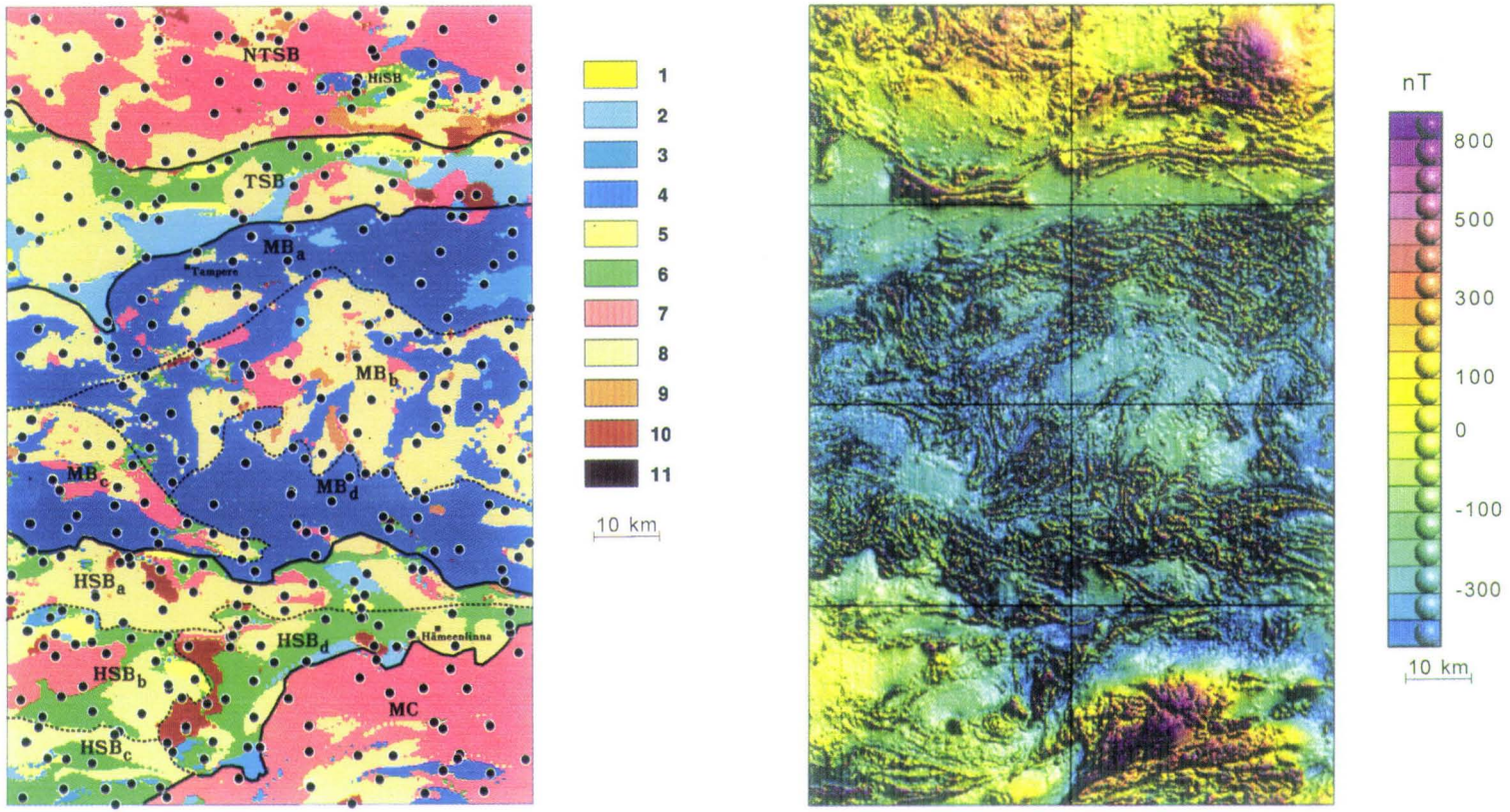

Fig. 2a. The study area shown as general geological map (left, Lahtinen 1996) and low-altitude aeromagnetic anomaly map (right, data from GSF). Symbols in the geological map: 1 – arkose, 2 – greywacke/phyllite/mica schist, 3 – mica gneiss, 4 – veined gneiss/migmatite, 5 – felsic volcanite, 6 – intermediate/mafic volcanite, 7 – granite, 8 – granodiorite, 9 – quartz diorite, 10 – diorite/gabbro, 11 – peridotite. NTSB – North of the TSB, TSB – Tampere Schist Belt, MB – Mica gneiss–migmatite Belt, HSB – Hämeenlinna Schist Belt, MC – Microcline granite Complex, HiSB – Hirsilä Schist Belt. The municipalities of Tampere and Hämeenlinna are indicated.

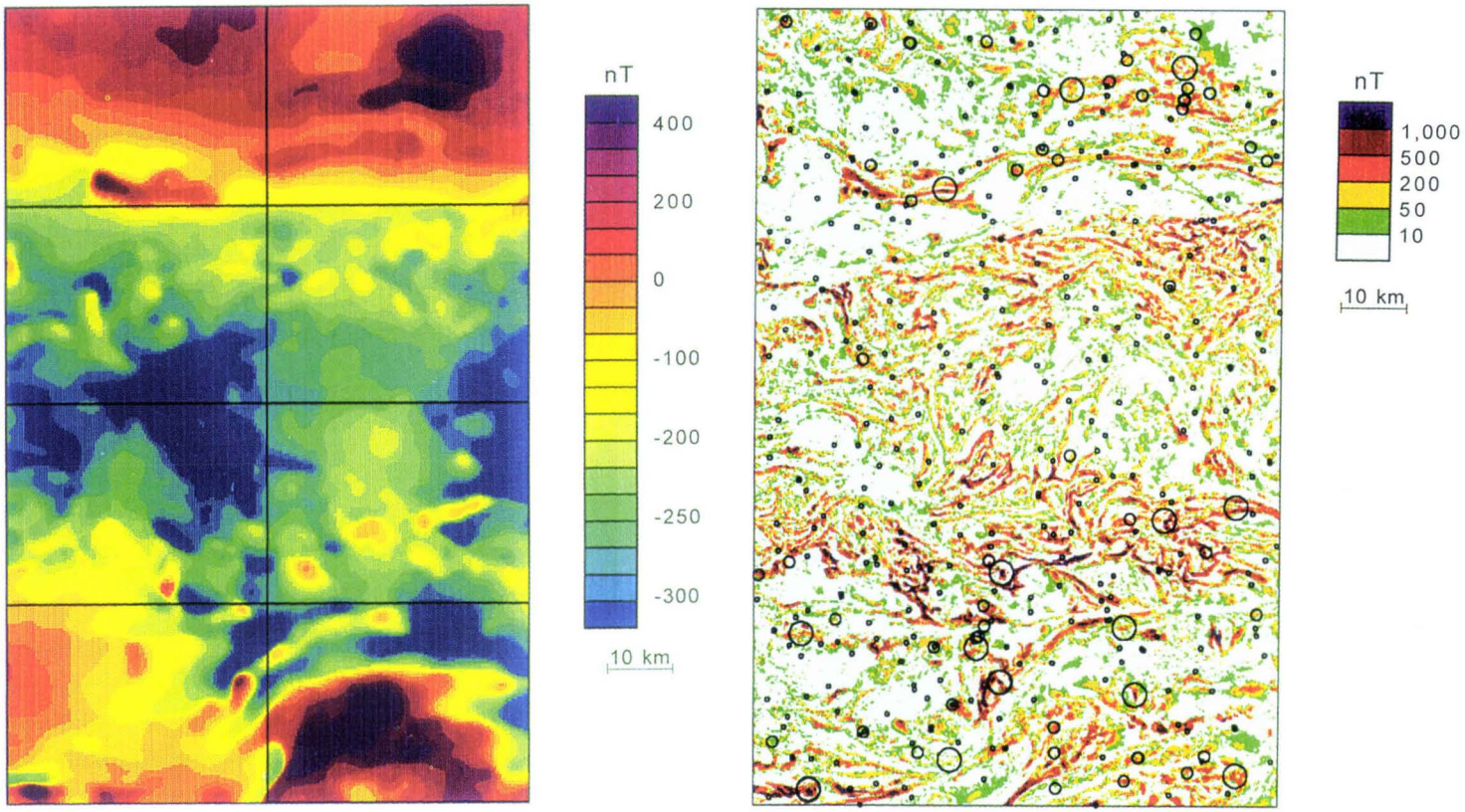

Fig 2b. The study area shown as smoothed aeromagnetic map (left) and residual map (right). The smoothed aeromagnetic map was produced by using a moving weighted median with 3 km radius for the data in the right figure in Fig. 2a. The residual map was produced by calculating the absolute value of the difference between the other two magnetic maps. It thus shows the amount of local deviation from the regional 'background'. Also negative deviations are shown as positive anomalies. Sampling sites and magnetization of samples are indicated with black dots. Small dots – samples producing slight magnetic fields ($J < 0.25$ A/m), medium-sized dots – samples producing weak magnetic fields (50–500 nT) for sheet-like bodies ($J = 0.25–2.5$ A/m), large dots – samples producing strong magnetic fields (>500 nT) for sheet-like bodies ($J > 2.5$ A/m) when sheet thickness is of the same order as the flight altitude.

sification (1996) of rock types into different groups has been adopted. The petrophysical register of the GSF normally contains data for one to three samples from one outcrop. To study the well-known feature that rocks of the same type may exhibit susceptibilities of different order of magnitude even when located nearby, twenty sample pairs (set B) with low and high magnetic susceptibilities were selected from the register and examined, to determine whether the divergence might be explained by differences in chemical composition or the nature of the opaque minerals. The temperature spectrum (i.e. temperature dependence) of the susceptibility was measured, and paramagnetic susceptibilities were calculated by Curie's law for selected (from set A) paramagnetic samples (24, set C) by applying the method of Hrouda (1994). The areal differences and the causes of the regional anomalies are discussed.

METHODS AND DEFINITIONS

The 403 samples described as set A, each consisting of four subsamples, were taken from the same lithological unit in a single outcrop according to the sampling strategy described by Lahtinen (1996). Sampling was done with a portable mini-drill with a diamond bit, or occasionally a large sledge hammer was used instead. The visibly weathered top of drill cores (usually 2–10 mm) was removed. Most of the chemical analyses were done in the chemical laboratories of the GSF at Espoo and Rovaniemi, with some trace elements measured at the Technical Research Centre of Finland and the XRAL laboratories in Canada. Detailed descriptions of the analytical methods and the precision and accuracy of the determinations can be found in Sandström (1996).

The petrophysical properties (all sets) were measured in the GSF Petrophysical Laboratory at Espoo. The equipment has been described by Puranen (1989). Rock bulk densities were determined by weighing the samples in air and water. The standard error of repeated density determinations was less than 2 kg/m^3. The porosity of crystalline rocks may create a systematic error, which is normally below 1%, however (Henkel 1976, Kivekäs 1993). The susceptibility data were measured with a susceptibility bridge K-3A (Puranen & Puranen, 1977), with standard errors of repeated measurements about 10^{-9} m^3/kg (2.5–$3 \cdot 10^{-6}$ SI) for weakly magnetic samples and about 2% for strongly magnetic samples (Puranen 1989). The intensity of natural remanent magnetization (NRM) was measured by R2 equipment (Puranen & Sulkanen, 1985) with remanence error less than 10% for average sample weights of 500 g. The threshold value is $20 \cdot 10^{-6}$ Am^2/kg, corresponding to values of 50–60 mA/m for volume magnetization of average Finnish rock densities.

The petrophysical properties of the set A rocks are calculated averages of two to six measurements made on the four subsamples of the same lithological unit. For about 130 samples, where subsample weights were from 100 to 500 g, four to six measurements were made on the group of subsamples. The other, approximately 270 samples, with subsample weights of only 50 to 100 g, were first checked with a magnetometer for their petrophysical properties and if one or more of the subsamples showed ferrimagnetic effects all four subsamples were measured. Otherwise, only two subsamples were measured. Since the sample weights of the 270 samples were smaller than normally used, the measurement errors were larger than noted above. However, averaging of the results from several subsam-

ples improved the reliability of the results. The heterogeneous nature of the migmatites produces wide variation between subsamples, and a heterogeneous distribution of magnetite likewise is the probable cause of the variation of magnetic properties in coarse-grained granitoids.

The parameters we measured were bulk density (D), volume susceptibility (k) and intensity of NRM (M), and from these we calculated mass susceptibility (X) and the Q-ratio. To estimate the ferrimagnetic contribution in samples belonging to a typical paramagnetic range, mass susceptibilities were divided into paramagnetic and ferrimagnetic components and the ferrimagnetic Q-ratio was calculated. Curie's law and chemically determined iron (assuming that all iron is ferric, Fe^{3+}) and manganese contents were used to calculate the chemically estimated paramagnetic mass susceptibility (Vernon 1961, Puranen 1989), which was further converted to chemically estimated paramagnetic volume susceptibility (k_{pc}). The k_{pc} value is normally slightly overestimated and gives the maximum value. The estimated ferrimagnetic susceptibility (k_{fc}) was calculated by subtracting the k_{pc} value from the measured volume susceptibility. Diamagnetic and antiferromagnetic effects were neglected. Some calculated k_{fc} values appeared to be negative due to estimation errors and were set to zero in Tables 2–3 and to 3 μSI ($\bullet 10^{-6}$ SI) in logarithmic susceptibility diagrams (Figs. 5, 8, 11 and 14). The amount of overestimation of k_{pc} is about 50–120 μSI in cases where the actual oxidation state is +2 and the diamagnetic minerals have interpreted values from -20 to -50 μSI for the whole sample. This maximum overestimation corresponds to c. 0.3 weight per cent of iron in silicates or to c. 0.003 weight per cent of magnetite.

Magnetically, Finnish Precambrian rocks are bimodal dividing into weakly and strongly magnetic populations called paramagnetic and ferrimagnetic by Puranen (1989). The populations are separated in such a way that the paramagnetic population is defined by the linear part of the average density–mass susceptibility diagrams. The boundary value varies from 22 to 52 $10^{-8}m^3/kg$ (X) for the different rock types and the relative abundance of the ferrimagnetic (strongly magnetic) population varies from 0.17 to 0.41 (F). The majority of magnetic anomalies visible on aeromagnetic maps are due to the strongly magnetic population (ferrimagnetic population). The weakly magnetic population (paramagnetic population) normally causes magnetic fields less than 50nT, but ferrimagnetic minerals are also present in this population and may cause higher intensities occasionally.

In this paper we define paramagnetic population differently, on a sample level. We say that a sample belongs to the paramagnetic population if its paramagnetic magnetization is greater than ferrimagnetic magnetization, and vice versa for samples belonging to the ferrimagnetic population. In this definition there is no single susceptibility value delimiting the populations. The definition is intended to serve magnetic anomaly interpretation. This division between populations depends on external field and temperature. If the former vanishes, practically all samples fall into the ferrimagnetic population. If the temperature exceeds the Curie temperature of all ferrimagnetic minerals in the sample, it falls into the paramagnetic population. The definition is independent of how well the weakly and strongly magnetic populations separate from each other in parameter space in different areas and rock types. However, there still remains a problem in terminology: since it contains a ferrimagnetic component of magnetization, although smaller in intensity than the paramagnetic component, a sample belonging to the paramagnetic population is not truely paramagnetic.

Twenty-four samples of the paramagnetic population (set C) were selected for more detailed study of the different components of magnetization. The selection was made by comparing the k_{pc} (see above) with the meas-

ured volume susceptibilities. A part of the stored drill cores were crushed with a ceramic jaw crusher and three quarters of the crushed portion was ground in a swing mill in a tungsten carbide grinding vessel. Magnetic susceptibility did not change during crushing, but during grinding it increased by about 50 μSI on average, probably due to cobalt since Co contamination up to 80 ppm was observed in the chemical analysis. The resultant powder was analysed for $Fe_{tot.}$ and Mn by ICP-AES, and for ferrous iron by titrimetric method. The remaining crushed portion (one quarter) was further ground in an agate mill and used for Curie-spectrum measurements by KLY-2 bridge and CS-2 robot. The Curmage program was used to control the measurements. Sample weight was 500 mg and preparate tubes were cleaned with hydrochloric acid between measurements. The calibration standard and the oven level up to 200°C were measured before measurement of the sample. The oven level was subtracted from the measured spectrum by the Cureval program, which also was used for calculations of thermally estimated paramagnetic mass susceptibilities according to the method of Hrouda (1994). The composite effect of ferrimagnetic and diamagnetic susceptibilities was calculated using bulk mass susceptibility and thermally estimated paramagnetic mass susceptibility reduced to room temperature. The thermally estimated ferrimagnetic mass susceptibility was further calculated by subtracting the effect of diamagnetic mass susceptibility obtained from a linear model of the density coupled diamagnetic susceptibilities of quartz and forsterite.

Definitions of the terms we employ are as follows:

– chemically estimated paramagnetic susceptibility (k_{pc}, see above)
– chemically estimated ferrimagnetic susceptibility ($k_{fc}=k-k_{pc}$)
– chemically estimated ferrimagnetic Q-ratio ($Q_{fc}=M/(0.041 \times k_{fc})$); for average Finnish field strength
– paramagnetic sample ($k_{fc} \leq 0$)
– ferrimagnetic sample ($k_{fc}>0$)
– paramagnetic population ($k_{fc} \leq k_{pc}$)
– ferrimagnetic population ($k_{fc}>k_{pc}$)
– thermally estimated paramagnetic mass susceptibility (X_{pt})
– thermally estimated ferrimagnetic mass susceptibility (X_{ft}, see above)
– mass susceptibility corrected for paramagnetic Mn (X_{Fe})

CORRELATIONS BETWEEN PETROPHYSICAL AND GEOCHEMICAL PROPERTIES

Sedimentary rocks

The geochemical division of the sedimentary rocks into eight groups (SG1–SG8) as described by Lahtinen (1996) is adopted in this study. Within these groups two main divisions are distinguished: arc-related (SG1) and basement-related (SG3–SG7) sedimentary rocks. The arc-related rocks are characterized by wide geochemical variation with a low degree of weathering in the source (low CIA values, Nesbitt & Young 1982), and the chemical composition is comparable to some extent with arc volcanics.

The basement-related sedimentary rocks (SG3–SG7) are derived from a more homogenized, weathered and mixed Archaean to Palaeoproterozoic source, with the groups showing gradational compositional change in the source area. The grain-size sorting of ferro-

magnesian minerals is a significant factor controlling the differences in composition (Lahtinen 1996). Groups SG3–SG4 include psammitic greywackes and mica gneisses, with SG4 representing a slightly more mafic source. SG5 samples are concentrated in the MB and appear to be of more silty to pelitic origin (now mainly migmatites) than the SG4. A more mafic source is indicated for at least some of the SG5 samples. Amounts of chemical and possibly also organic sedimentation are higher, which leads to lower SiO_2 values and higher contents of sulphide-related elements. SG6–SG7 are pelitic rocks (often migmatites) with SG6 having the more mafic source. Black schists are considered as a subgroup of pelites, as are the high-grade SG7 migmatites from the MC. The latter are migmatites with granitic leucosomes, which differ from the predominantly tonalitic migmatites in the MB. The SG2 group comprises five samples with indications of a more mafic source than the other groups (excluding some SG1 samples), and SG8 comprises four mafic greywackes not directly related to any of the other groups (ibid.). These two groups have been excluded from the section sedimentary rocks in Table 3.

Differences in density are normally due to differences in the amount of ferromagnesian minerals. The most abundant ferromagnesian mineral in the sedimentary samples is biotite, which varies widely in density from 2700 to 3300 kg/m^3, with normal variation from 2860 to 3150 kg/m^3 (Deer et al. 1962b). The most abundant light minerals are quartz and plagioclase (normally oligoclase). The average densities of 3000 kg/m^3 for biotite and 2650 kg/m^3 for both quartz and plagioclase (An 18), as approximated from Deer et al. (1962b, 1963b), have been used to construct a mixing line (Fig. 3). Since in reality the density of biotite varies, the line represents only one possible mixing line. Like biotite, also chlorite varies in density. The occurrence of K-feldspar lowers the density and puts such samples below the mixing line. The increase of an anorthite component in plagioclase and the occurrence of hornblende, on the other hand, push the samples to higher density values. The same effect is produced by metamorphic minerals such as garnet, sillimanite, andalusite and muscovite, but cordierite is of lower density, and cordierite is the other main mineral besides K-feldspar lowering the density in metasedimentary rocks (Fig. 3). Unfortunately, varying metamorphic conditions produce a highly complex mineralogy in some rocks, pelites in particular. Andalusite and muscovite are often found in amphibolite facies pelites, but abundant K-feldspar and sillimanite characterize pelites of a higher metamorphic grade. The heterogeneity of migmatites produces scatter (Fig. 3), especially where only two subsamples were measured.

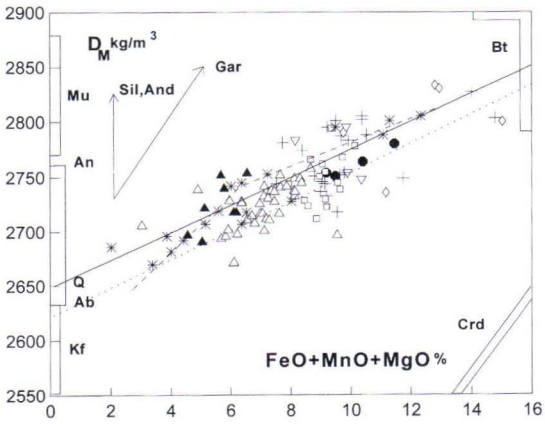

Fig. 3. D_M versus FeO+MnO+MgO diagram for sedimentary rocks in the Tampere–Hämeenlinna area. Data from this study. D_M is the measured bulk density (D) corrected with the average porosity (10 kg/m^3, Kivekäs 1993). The density of minerals from Deer et al. (1962a, 1962b, 1963a, 1963b). Mu – muscovite, An – anorthite, Q – quartz, Ab – albite, Kf – K-feldspar, Bt – biotite, Crd – cordierite, Sil – sillimanite, And – andalusite and Gar – garnet. Solid line – hypothetical biotite versus quartz+plagioclase (An 18) mixing line, dashed line – approximated trend for SG1 sediments and dotted line – approximated trend for major part of SG3 sediments. Asterisks – SG1, open diamonds – SG2, filled upright triangles – SG3 and SG4 samples from the TSB, open upright triangles – other SG3 and SG4 samples, squares – SG5, crosses – SG6 and SG7 samples (excluding the MC samples), black circles – SG7 samples from the MC and open inverted triangles – SG8 samples.

The general trend for SG1 samples is shown by the dashed line in Fig. 3. The most mafic samples contain abundant hornblende, and also more anorthite-rich plagioclase than other samples, which increase the density. The occurrence of K-feldspar in turn lowers the density when going to more felsic samples. The three samples deviating to lower densities are a sheared rock and two samples with abundant K-feldspar. Three SG2 samples lie above the mixing line, two of them containing hornblende and one abundant garnet with biotite.

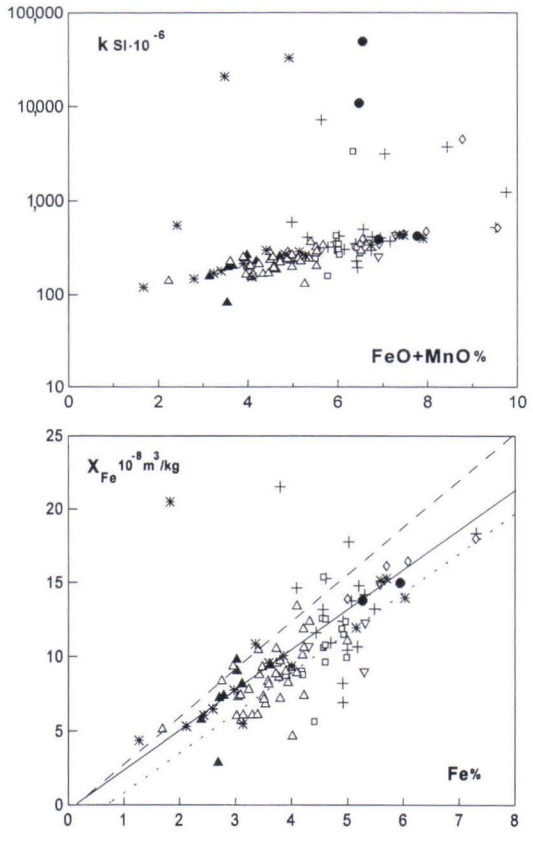

Fig. 4. Volume susceptibility (k) versus FeO+MnO diagram (upper figure) for sedimentary rocks in the Tampere–Hämeenlinna area, and mass susceptibility (X_{Fe}) versus Fe diagram (lower figure) for sedimentary rocks having k<1000 μSI. Data from this study. X_{Fe} is mass susceptibility minus the contribution from Mn, calculated by the formulas given in Puranen (1989). See Fig. 3 for symbols. Lower figure: solid line – paramagnetic Fe relation when total Fe as Fe^{2+} and diamagnetic minerals have an average mass susceptibility value of -0.5 ($10^{-8}m^3/kg$), dashed line – same situation but total Fe as Fe^{3+} and dotted line – similar to solid line, but diamagnetic minerals have an average mass susceptibility value of -2 ($10^{-8}m^3/kg$).

In addition to quartz, plagioclase and biotite, the basement-related psammitic greywackes and mica gneisses (SG3–SG4) contain muscovite locally, a small amount of K-feldspar and, in some more mafic samples, garnet. The most felsic sample is of increased density due to abundant metamorphic labradotitic plagioclase. The other felsic samples of higher density, especially the TSB samples, contain abundant muscovite.

Higher density SG5 sedimentary rocks have slightly higher CIA values (60–65) while lower density samples have lower CIA values (<60). The high density pelitic samples (SG6–SG7) tend to have high CIA values (65–70) and lack K-feldspar, while the presence of biotite+muscovite±andalusite/sillimanite±garnet increases the density. The lower density samples in SG6–SG7 normally have lower CIA values (60–65) and at least some of them contain metamorphic K-feldspar. The four SG7/MC samples have biotite, garnet, cordierite±sillimanite and three of the four K-feldspar, which gives them slightly lower densities.

The susceptibility data indicate a predominance of the paramagnetic population (for all sedimentary rocks 91%, Table 3), which is considered here first. The mass susceptibility versus Fe diagram in Fig. 4 shows a scattered relationship between these variables. The points deviating to lower values represent cases where only two subsamples were measured. One problem with the mass susceptibility (X_{Fe}) versus Fe diagram is the difficulty in determining the diamagnetic susceptibilities, which means that the diagram cannot be used to calculate the exact oxidation ratio.

The diagrams of intensity of NRM versus susceptibility and chemically estimated ferrimagnetic susceptibility (Fig. 5) show a division of the high susceptibility samples into two groups, where the samples with high Q-ratio (9–20) and elevated sulphur contents

form the pyrrhotite-bearing group and those with low Q-ratio (0.2–4) and low sulphur contents the magnetite-bearing group. A notable feature is that in most cases the elevated sulphur contents in the sedimentary rocks are due to paramagnetic pyrite or antiferromagnetic pyrrhotite. There are four black schist samples with about 1–2% S and 1.5–2.0% $C_{Graf.}$ and three of them contain pyrrhotite, while one contains only pyrite. Two of the SG1 samples exhibit high susceptibilities, and low S contents (<70 ppm) and Q-ratios <4, suggesting the presence of magnetite. Both samples are from the HiSB and probably are derived from the surrounding volcanics (Lahtinen 1996), which would indicate the primary nature of the magnetite.

The migmatites from the MC are totally devoid of graphite, which has been interpreted to be due to loss during migmatization

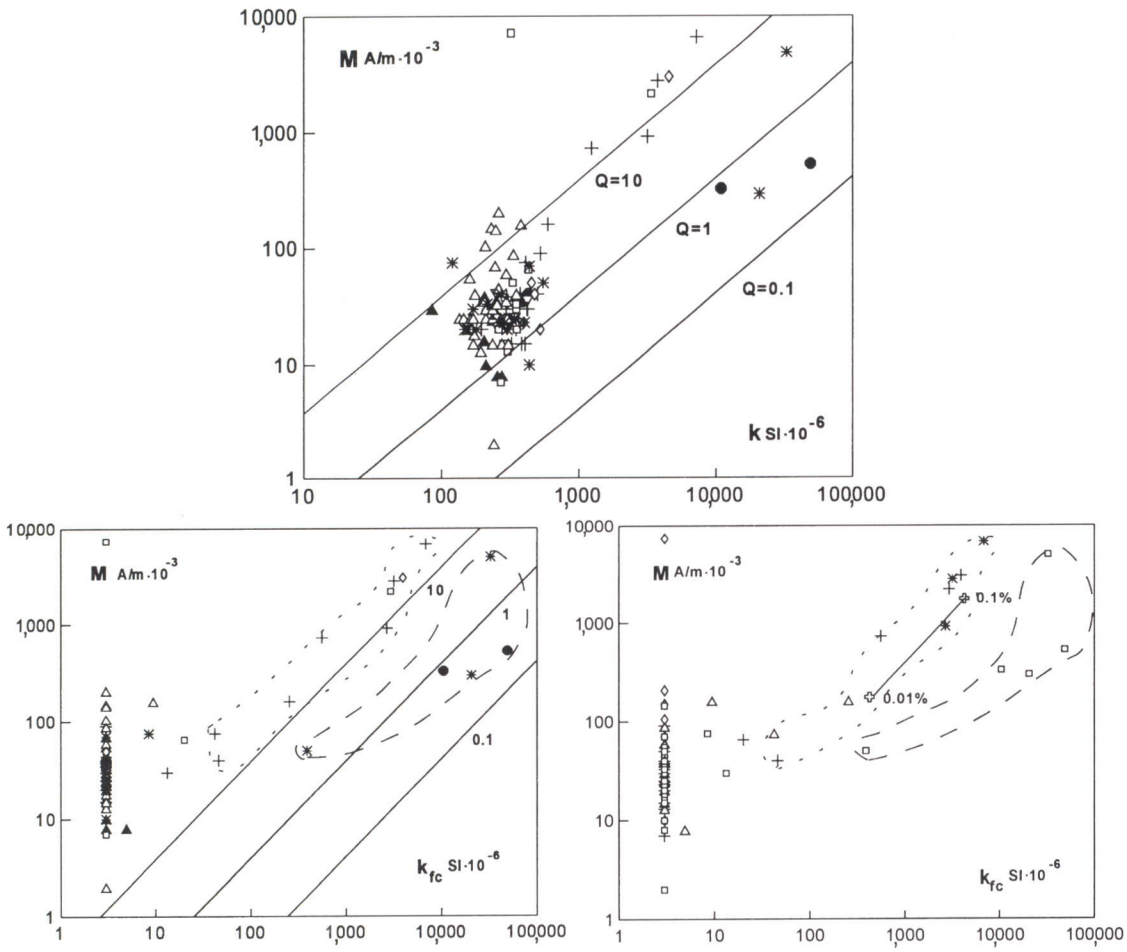

Fig. 5. Diagrams of intensity of NRM (M) versus volume susceptibility (k) (upper figure) and chemically estimated ferrimagnetic susceptibility (k_{fc})(lower figures) for sedimentary rocks in the Tampere–Hämeenlinna area. Data from this study. See Figure 3 for symbols in upper and lower left figures. Q-ratios are indicated in upper figure and estimated Q_{fc}-ratios for ferrimagnetic susceptibilities are indicated in the lower left diagram. Symbols in lower right figure: open squares – samples <200 ppm S, open diamonds – 200–500 ppm S, open triangles – 500–1000 ppm S, crosses – 1000–10000 ppm S and asterisks – black schists about 1–2% of S and of $C_{Graf.}$. The line indicates the contribution from 0.01% to 0.1% of sulphur calculated as pyrrhotite with susceptibility of 1,575,000 μSI and Q-ratio of 10. Lower figures: dashed line – 'magnetite' field, dotted line – 'pyrrhotite' field.

(Lahtinen 1996). At the same time, there has been a depletion of S and some sulphur-related elements. The two samples with high susceptibilities have lower S (<200 ppm) than the other two samples (250–550 ppm S), but otherwise there are no clear geochemical differences. The sample having highest susceptibility (Fig. 5) also has the lowest S value (94 ppm). Its mineralogy of cordierite+biotite+garnet+sillimanite+K-feldspar is indicative of near or granulite facies metamorphic conditions. The ferrimagnetic mineral (magnetite) seems to be concentrated in the cordierite-rich parts of the sample. A metamorphic origin in slightly oxidized conditions is proposed for the magnetite in these two high susceptibility samples, where the earlier reducing agents, graphite and sulphides, have been lost during migmatization.

The intensity of the NRM data (Fig. 5) shows the occurrence of samples with increased remanence without any clear increase in susceptibility values. The SG5 sample with very high remanence demonstrates the irregular behaviour of the remanence in some cases. There are two subsamples with values 14530 mA/m and 50 mA/m. The latter value falls within the main scatter of weakly magnetic samples.

Volcanic rocks

The division of the volcanic rocks into eight geochemical groups (VG1–VG8) (Lahtinen 1996) is also adopted here. VG1–VG4 comprise mainly mafic rocks of tholeiitic affinity and VG5–VG7 comprise intermediate to felsic rocks of calc-alkaline to shoshonitic affinity.

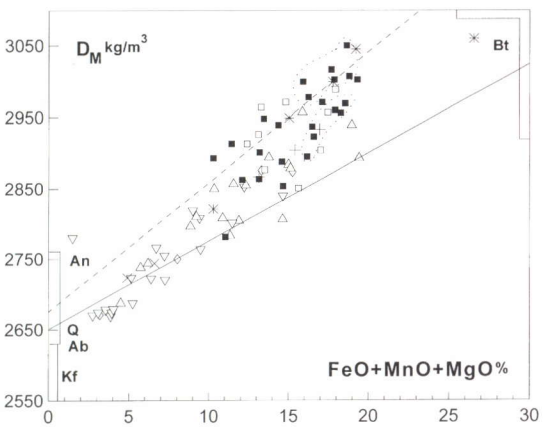

Fig. 6. D_M versus FeO+MnO+MgO diagram of volcanic rocks in the Tampere–Hämeenlinna area. Data from this study. Solid line – hypothetical biotite mixing line (see Fig. 3), dashed line – hypothetical hornblende mixing line. An – anorthite, Q – quartz, Ab – albite, Kf – K-feldspar, Bt – biotite. Asterisks – VG1, open squares – VG2, filled squares – VG3, crosses – VG4, open upright triangles – VG5, open inverted triangles – VG6, open diamonds – VG7 and diagonal crosses – VG8. Dotted fields enclose high and low density populations of mafic VG3 rocks.

VG1 is a composite group of five samples varying from mid-ocean ridge basalts (MORB) to within-plate basalts (WPB). Four of the samples are from the MB and one is from the Haveri formation in the TSB. Groups VG2–VG3 represent the rift-related Häme group (Hakkarainen 1994, Lahtinen 1996) in the HSB. The VG4 group is composed of three hypabyssal dykes of alkaline WPB affinity from the MB. Low-K to medium-K calc-alkaline rocks, mainly from the HSB, make up group VG5, and medium-K to high-K calc-alkaline rocks mainly from the TSB and HiSB make up VG6. Groups VG5–VG7 are subduction-related island arc rocks of mature continental island arc or Active Continental Margin (ACM) origin (Lahtinen 1996). Two tholeiitic dacites make up VG8 and they are excluded from the volcanic rocks in Table 3.

The density variation of the volcanic samples is shown in Fig. 6, against theoretical biotite and hornblende mixing lines. The one felsic VG6 sample deviating strongly to higher density is an altered rock with abundant muscovite and tourmaline. The felsic samples lighter than the biotite mixing line contain biotite as main ferromagnesian mineral, with

Table 1. Mean values and standard deviations for elements having t-test (SPSS Inc. 1988) probability <0.1 for the VG3 low (6 samples) and high (6 samples) density tholeiitic volcanic rocks shown as fields in Fig. 6. Bulk density (D), susceptibility (k) and intensity of NMR (M) data are included.

	Low density		High density		Pooled	Separate
	Mean	STD	Mean	STD	probability	probability
FeO%	10.54	0.40	11.50	1.16	0.083	0.102
FeO/MgO	1.61	0.21	2.05	0.50	0.074	0.089
MnO%	0.18	0.005	0.21	0.016	0.002	0.007
CaO%	9.30	1.09	10.68	1.32	0.077	0.078
Cu ppm	132.2	61.8	56.8	51.1	0.044	0.045
D kg/m^3	2930.0	27.6	2999.3	23.8	0.001	0.001
k SI·10^{-6}	18,711	28,083	2,857.5	4,816.5	0.203	0.228
M A/m·10^{-3}	312.2	388.6	124.7	184.7	0.311	0.320

K-feldspar present at least in some samples. The normal situation for intermediate rocks is the occurrence of both biotite and hornblende, with an increasing amount of hornblende in more mafic samples. Figure 6 is in agreement with this. VG4–VG8 samples are almost always lighter than the hornblende mixing line, which is also in agreement with the mineralogy of these samples.

Rocks denser than the hornblende mixing line are tholeiitic rocks and richer in iron. Normally they contain hornblende with locally occurring pyroxene, but many also contain biotite. The higher density values are proba-

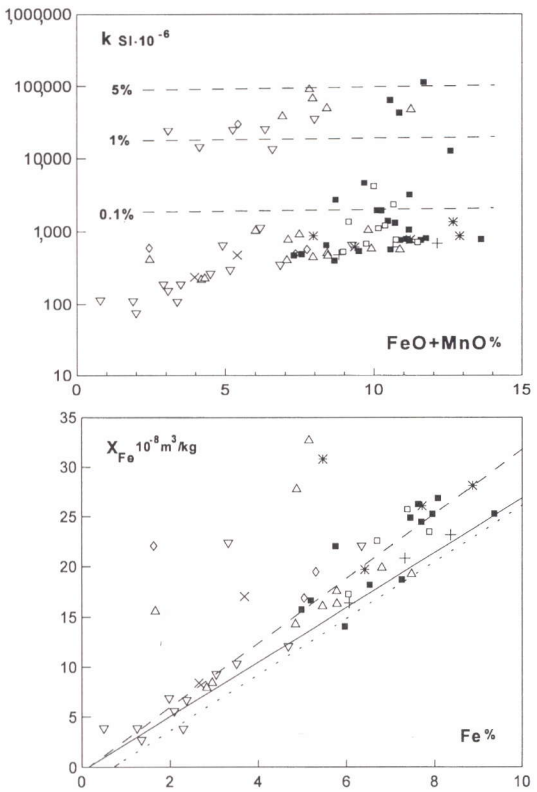

Fig. 7. Volume susceptibility (K) versus FeO+MnO diagram (upper figure) for volcanic rocks in the Tampere–Hämeenlinna area, and mass susceptibility versus Fe diagram (lower figure) for volcanic rocks having k<1000 µSI. Data from this study. X_{Fe} is mass susceptibility minus the contribution from Mn, calculated by the formulas given in Puranen (1989). See Fig. 6 for symbols. The dashed lines with numbers in upper diagram indicate the magnetite content (wt%) calculated by formula given in Puranen (1989). Refer to Fig. 4 for lines in lower diagram.

bly due to differences in the composition of biotite and hornblende, because the more iron-rich varieties of these minerals tend to be of higher density (Deer et al. 1962b, 1963a). Many of the VG3 samples are of lower density, and the more mafic of these (SiO_2 <53%) are shown as dotted field (Fig. 6). The other VG3 samples of lower density values are of more intermediate character (>54% SiO_2).

Table 1 summarizes the results of t-tests carried out with SPSS-X (SPSS Inc. 1988) to discover the differences in group means between the two sets of outlined VG3 samples (Fig. 6). The lower FeO/MgO ratio for the lower density samples indicates a slight difference in the composition of the ferromagnesian minerals. The higher Cu, combined with the lower CaO, could be the result of slight

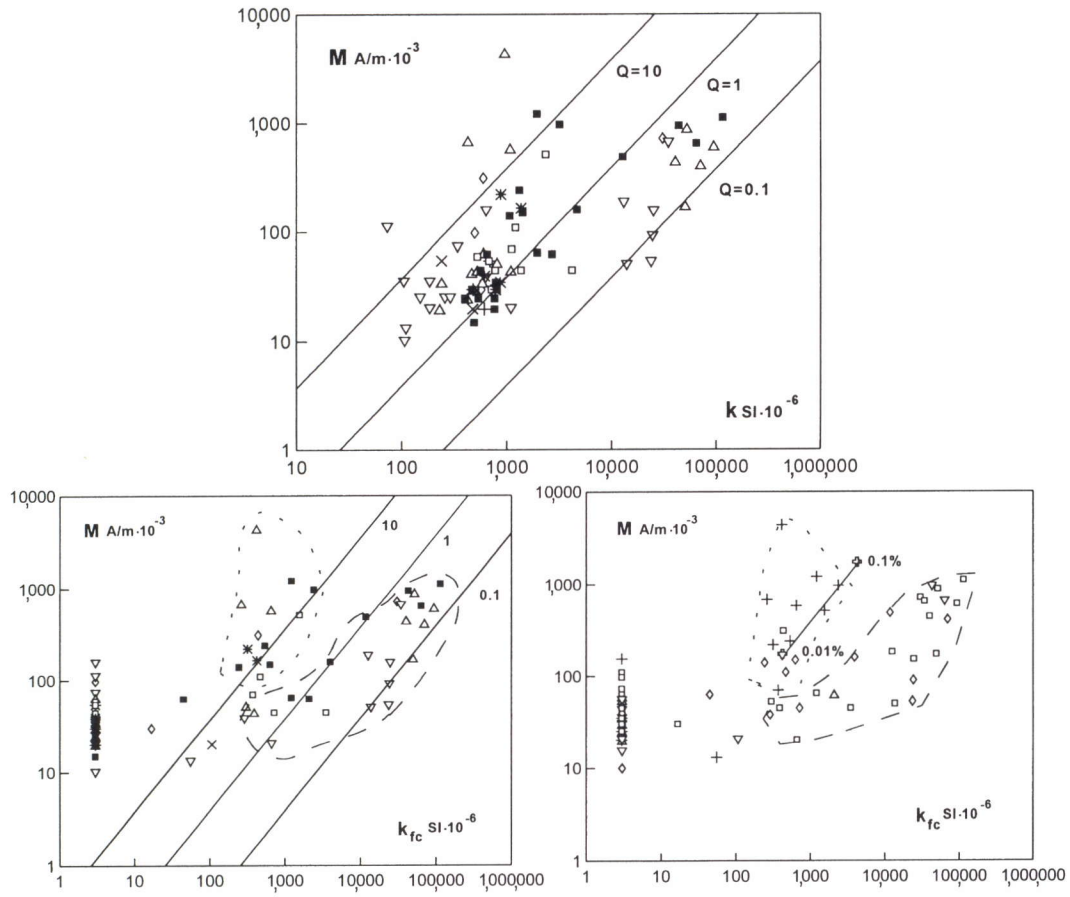

Fig. 8. Diagrams of intensity of NRM (M) versus volume susceptibility (k) (upper figure) and chemically estimated ferrimagnetic susceptibility (k_{fc}) diagrams (lower figures) for volcanic rocks in the Tampere–Hämeenlinna area. Data from this study. See Fig. 6 for symbols in upper and lower left figures. Q-ratios are indicated in upper figure and chemically estimated Q_{fc}-ratios for ferrimagnetic susceptibilities in the lower left figure. Symbols in lower right figure: open squares – samples <100 ppm S, open diamonds – 100–200 ppm S, open inverted triangles – 200–500 ppm S, open upright triangles – 500–1000 ppm S and crosses – >1000 ppm S. The line indicates the contribution from 0.01% to 0.1% of sulphur calculated as pyrrhotite with susceptibility of 1,575,000 μSI and Q-ratio of 10. Lower figures: dashed line – 'magnetite' field, dotted line – 'pyrrhotite' field.

alteration and mineralization, causing a change in the mineral composition. At least in part, however, these features are associated with the more differentiated nature of the samples.

The susceptibility data are visualized in Figure 7, where 65% of the samples belong to the paramagnetic population (Table 3). The lower diagram shows a plot of the low susceptibility samples (Fig. 7). The correlation of mass susceptibility (X_{Fe}) and Fe is good, and the samples with mass susceptibilities slightly above the estimated paramagnetic trend can be interpreted to contain small amounts of ferrimagnetic sulphides or a minute amount of other ferrimagnetic minerals as inclusions in ferromagnesian minerals.

Figure 8 shows plots of the intensity of NRM versus magnetic susceptibility and chemically estimated ferrimagnetic susceptibility (k_{fc}). 'Magnetite' and 'pyrrhotite' fields are shown in outline, though some of the low sulphur samples in the 'pyrrhotite' field may indicate the presence of martite/hematite. The separation between the two fields is distinct at higher k_{fc} values, but at lower values they partially overlap. In general, the VG1–VG2 samples follow the paramagnetic trend (Fig. 7), and the deviations to higher susceptibility values are due to increase in S and the Q-ratio (Fig. 8), pointing to the presence of pyrrhotite. Two of the VG2 samples appear to contain a different ferrimagnetic mineral (magnetite).

Two of the VG3 samples have elevated susceptibilities associated with high S (>0.1%) and elevated Q-ratios (>5) indicating the occurrence of pyrrhotite (Fig. 8). Seven VG3 samples plot in the 'magnetite' field, four of them with an abundant occurrence of magnetite. Three form the trachybasalt subgroup in the VG3 and the fourth has high K, possibly due to crustal contamination (Lahtinen 1996).

All three VG4 samples are paramagnetic in the sense defined on page 14 and show a linear trend at rather low levels (Fig. 8), possibly indicating a low oxidation ratio. This is supported by the occurrence of a small amount of graphite in one sample, suggesting an overall reducing environment.

VG5 samples divide into paramagnetic samples (8 samples), samples with pyrrhotite (3 samples), magnetite-bearing samples (6 samples) and samples (one) with a minute amount of ferrimagnetic minerals (Fig. 8). Two of the magnetite-bearing samples are tuff breccias, one is a lapilli-tuff and one is a banded amphibolite probably of pyroclastic origin.

There are 19 VG6 samples, with nine samples showing the occurrence of a ferrimagnetic component. Six samples exhibit high susceptibilities with normally low Q-ratios (Figs. 7 and 8), indicating the occurrence of coarse magnetite. All four samples from the HiSB exhibit strong ferrimagnetism.

The shoshonite group VG7 comprises two samples in the paramagnetic population, one sample in the 'pyrrhotite' field and one sample in the 'magnetite' field (Fig. 8). The sample in the 'pyrrhotite' field has a very low S value of 59 ppm and thus the occurrence of hematite/martite or fine-grained magnetite is more probable than pyrrhotite. The magnetite-bearing sample is more differentiated than the two paramagnetic samples, and the sample in the 'pyrrhotite' field is the most differentiated.

There are some paramagnetic volcanic samples with elevated intensity of NRM values but no clear chemical differences to account for this. The VG6 paramagnetic sample with highest average remanence (155 mA/m) exhibits variation from 0 mA/m to 550 mA/m in the four subsamples demonstrating the irregular behaviour of the intensity of NRM.

Plutonic rocks

Mafic plutonic rocks

The mafic plutonic rocks have been considered on an areal basis only (Lahtinen 1996). Most of the mafic plutonic rocks are characterized by a simple mineralogy of hornblende, biotite and plagioclase. This is also seen in the density diagram (Fig. 9), where most of the samples plot between the hornblende and biotite mixing lines. Some of the samples contain only a small amount of biotite, however, and plot near the hornblende mixing line. Samples above or near to the hornblende mixing line often also contain pyroxene, and the sample from the MB also contains abundant garnet. Cummingtonite and chlorite are present in some samples.

The susceptibility data indicate a paramagnetic nature for most of the mafic plutonic samples (Fig. 10). Of the ten samples from the NTSB, three plot in the 'magnetite' field (Fig. 11). The two samples with highest susceptibilities are enriched in K, Ba, Th, La, P, Ti and Zr, indicative of alkaline WPB affinity (Lahtinen 1996). Both samples are highly differentiated rocks and the occurrence of magnetite with abundant biotite could point to higher water content with oxidizing conditions in highly differentiated magma. The other possibility is an interaction with felsic magmas to increase the water content and oxygen fugacity.

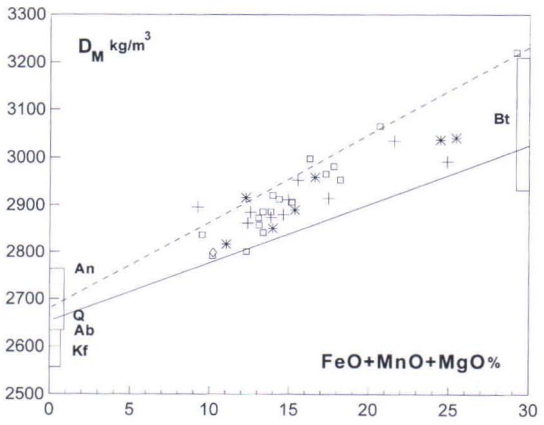

Fig. 9. D_M versus FeO+MnO+MgO diagram of mafic plutonic rocks in the Tampere–Hämeenlinna area. Data from this study. Solid line – hypothetical biotite mixing line (see Fig. 3), dashed line – hypothetical hornblende mixing line. An – anorthite, Q – quartz, Ab – albite, Kf – K-feldspar, Bt – biotite. Crosses – samples from the NTSB, open diamonds – samples from the TSB, asterisks – samples from the MB and open squares – samples from the HSB.

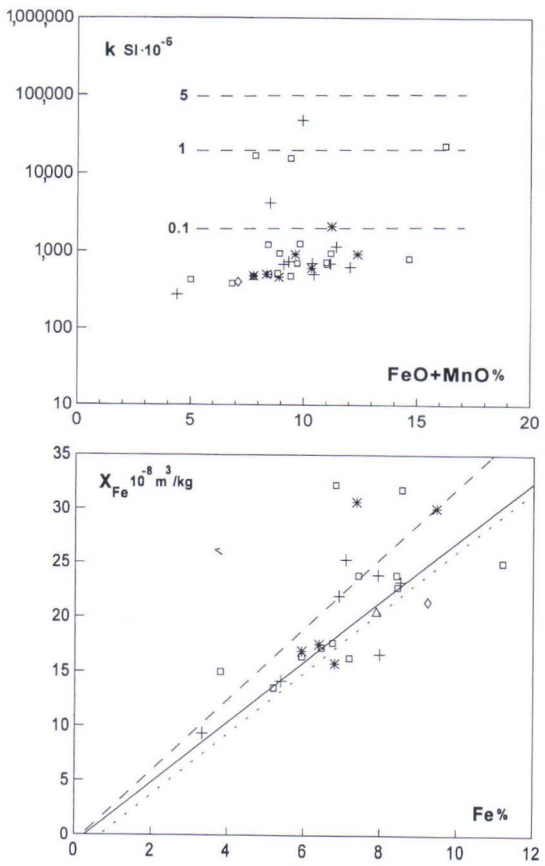

Fig. 10. Volume susceptibility (k) versus FeO+MnO diagram (upper figure) for mafic plutonic rocks in the Tampere–Hämeenlinna area, and mass susceptibility (X_{Fe}) versus Fe diagram (lower figure) for mafic plutonic rocks having k<1000 μSI. Data from this study. X_{Fe} is mass susceptibility minus the contribution from Mn, calculated by the formulas given in Puranen (1989). See Fig. 9 for symbols. The dashed lines with numbers in upper figure indicate the magnetite contents (wt%) calculated by formula given in Puranen (1989). Refer to Fig. 4 for lines in lower figure.

Two of the mafic plutonic samples from the MB plot in the 'pyrrhotite' field (Fig. 11), and pyrrhotite was visually observed in the sample with higher sulphur content. The other four samples are paramagnetic. There are four samples from the HSB plotting in the 'magnetite' field and two of them have elevated susceptibilities. Both samples differ from the normally tholeiitic mafic plutonics in their calc-alkaline character (Lahtinen 1996). The other sample with high susceptibility is of comingled nature and shows signs of interaction with granodiorite melt. The sample with highest value of the intensity of NRM in Fig. 11 again demonstrates the irregular behaviour of remanence, as evident in the two subsample values of 390 and 10,870 mA/m with associated susceptibility values of 17,230 and 28,390 μSI. The small amount of sulphides relative to the high susceptibility value indicates the occurrence of magnetite, but it is not clear whether the high remanence value of the one subsample is due to difference in grain-size or to some other factor.

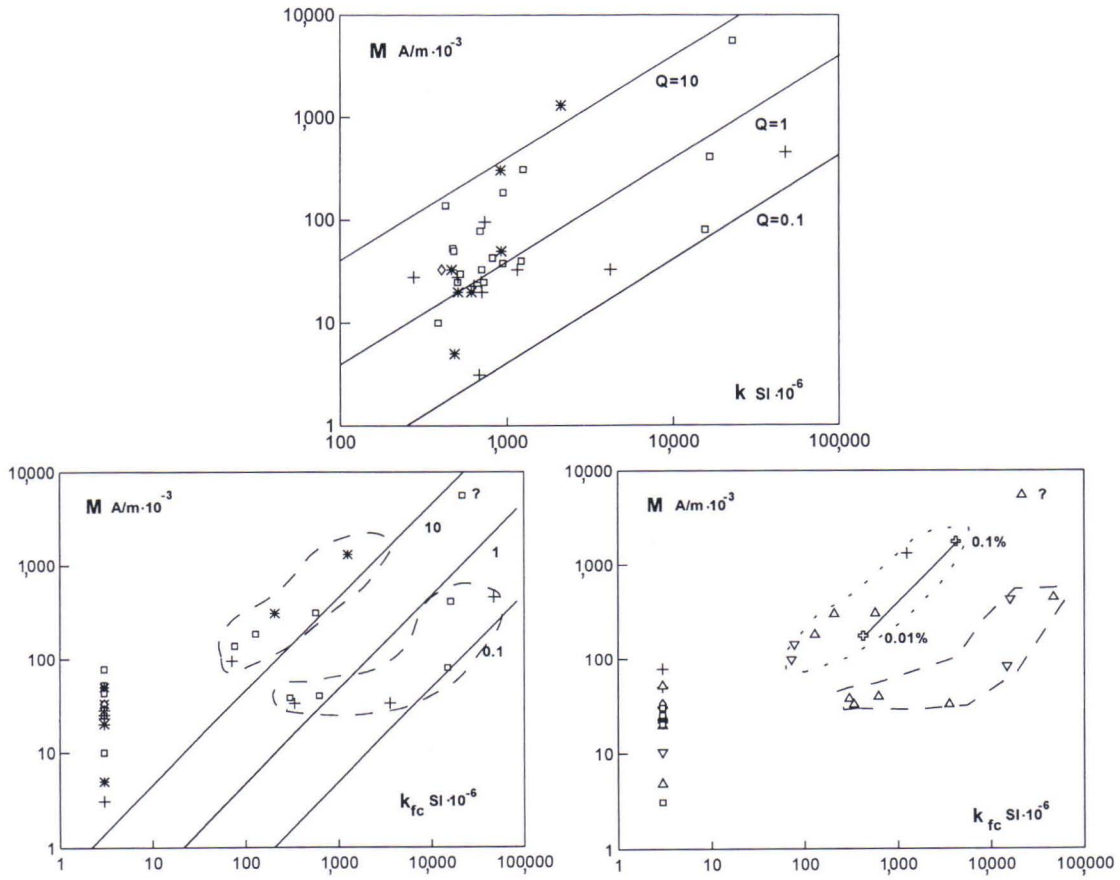

Fig. 11. Diagrams of intensity of NRM (M) versus susceptibility (k) (upper figure) and chemically estimated ferrimagnetic susceptibility (k_{fc}) diagrams (lower figures) for mafic plutonic rocks in the Tampere–Hämeenlinna area. Data from this study. See Fig. 9 for symbols in upper and lower left figures. Q-ratios are indicated in upper figure and chemically estimated Q_{fc}-ratios for ferrimagnetic susceptibilities in the lower left figure. Symbols in lower right figure: open squares – samples <200 ppm S, open inverted triangles – 200–500 ppm S, open upright triangles – 500–1000 ppm S and crosses – >1000 ppm S. The line indicates the contribution from 0.01% to 0.1% of sulphur calculated as pyrrhotite with susceptibility of 1,575,000 μSI and Q-ratio of 10. Lower figures: dashed line – 'magnetite' field, dotted line – 'pyrrhotite' field.

Granitoids

The granitoids have been geochemically divided into eight general classes GG1–GG8 (Lahtinen 1996). The GG7 group shows S-type characteristics, while the other groups are of I-type, although GG3 and GG8 have some S-type characteristics due to assimilated sedimentary material. High-K calc-alkaline granitoids, comprising the three groups GG1–GG3, are the most abundant rock type. The GG1 rocks are high-K calc-alkaline granitoids from the NTSB, possibly cogenetic with volcanics. The GG2 group, with its areal subgroups, consists of normal high-K calc-alkaline granitoids, and the GG3 group of high-K calc-alkaline granitoids with an assimilated sedimentary component. Group GG4 consists of medium-K calc-alkaline granitoids, and the GG5 group of felsic high-K granites from the NTSB with variable calc-alkaline to mainly tholeiitic affinities. The very high-K GG6 granites of tholeiitic affinity are mainly confined to the NTSB, and the GG6 granites from the HSB are considered as a subgroup (see Lahtinen 1996). The GG7 rocks comprise microcline granites from the MC and small plutons and pegmatites from the MB. GG8 granitoids, mainly from the MB, are high-TiO_2 granitoids of tholeiitic affinity often associated with an assimilated sediment component. Groups GG1–GG4 (excluding GG3 Nokia-type) are considered as syn-tectonic (1.89–1.88 Ga) and groups GG5–GG6 and GG3 Nokia-type and at least the main part of the GG8 rocks are late- to post-tectonic, related to the 1.89–1.88 Ga collision. The GG7 granites in the MC are younger (1.84–1.81 Ga) and associated with the proposed 1.86–1.84 Ga collision (Lahtinen 1996).

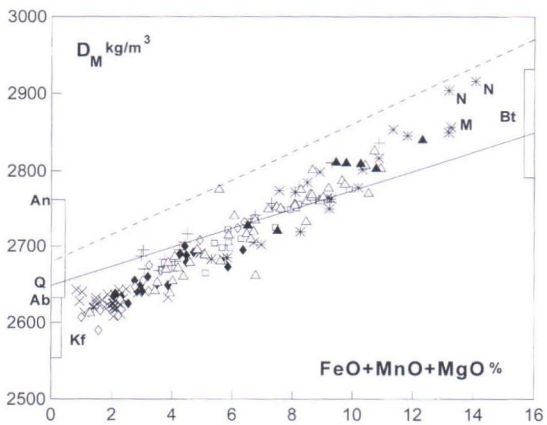

Fig. 12. D_M versus FeO+MnO+MgO diagram of granitoids in the Tampere–Hämeenlinna area. Data from this study. Solid line – hypothetical biotite mixing line, dashed line – hypothetical hornblende mixing line. An – anorthite, Q – quartz, Ab – albite, Kf – K-feldspar, Bt – biotite. Filled triangles – GG1, open triangles – GG2, open squares – GG3, crosses – GG4, open diamonds – GG5, filled diamonds – GG6, diagonal crosses – GG7 and asterisks – GG8. N – samples from the NTSB and M – sample from the MC referred to in text

The density diagram (Fig. 12) shows a relatively good correlation between density and the contents of ferromagnesian elements. There is a change from hornblende-bearing mafic samples with biotite to intermediate samples with predominantly biotite. At the same time, the amount of K-feldspar increases and it is the most abundant mineral with biotite in the most felsic samples. This accords well with the observed mineralogy. The medium-K granitoids (GG4) contain less K-feldspar, as seen in the deviation of these samples to slightly higher densities. The assimilated high-K calc-alkaline group (GG3) normally contains only biotite, unlike the normal high-K calc-alkaline group (GG2) which also contains hornblende, and there is a tendency for GG3 samples to be of slightly lower density (Fig. 12). The GG8 samples with lower densities tend to have a larger assimilation component, which is reflected in both the chemical and the mineralogical composition. The microcline granites deviating to higher densities contain not only biotite but muscovite and garnet, which give them higher densities.

About 70% of the granitoid samples have only paramagnetic properties (Fig. 13, Table 3). In general these follow the calculated mass susceptibility versus iron trends, but there is also a deviation to lower values, perhaps indicating differences in the diamagnetic miner-

als. According to Fig. 14, the increase in susceptibility usually cannot be due to pyrrhotite, though some samples with slightly increased ferrimagnetic susceptibility may contain a minute amount of pyrrhotite. The samples outside the 'magnetite' field ($Q \leq 1$) in Fig. 14 contain either hematite/martite or very fine-grained magnetite. Martite is very common in granitoids as seen in Table 2.

There are seven GG1 samples, of which three plot in the 'magnetite' field. One of these three is an orthogneiss and the other two show indications of comingling with mafic magma, which may be the cause of the magnetite crystallization. Of the 45 samples in the GG2, seven plot in the 'magnetite' field (Fig. 14). At least one of them is of hybrid origin, but there are no clear geochemical differences between the other ferrimagnetic samples and the paramagnetic samples.

The assimilated high-K calc-alkaline group GG3 consists of 16 samples and there is only one sample, from the MC, plotting in the 'magnetite' field (Fig. 14). This sample contains abundant mafic enclaves and is also granitized.

Of the 19 medium-K calc-alkaline samples (GG4), six plot in the 'magnetite' field (Fig. 14) and four of the six are from the MC. Two of the MC samples are granodiorites of tholeiitic affinity and are considered as a GG4 subgroup (Lahtinen 1996). The third MC sample contains abundant mafic enclaves and is hybrid in nature. The fourth is a strongly foliated and shear banded granodiorite. The remaining 'normal' medium-K calc-alkaline granitoids are paramagnetic.

There are 13 samples of high-K granitoids (GG5) occurring in the NTSB and only one of these is paramagnetic (Fig. 14). The elevated remanence, producing higher Q values (Fig. 14), indicates the occurrence of hematite (martite) and/or very fine-grained magnetite. The very high-K group GG6 consists of 18 samples, of which six are paramagnetic and four of these from the HSB subgroup. The other 14 samples are from the NTSB (one from TSB) and, according to Fig. 14, rather coarse-grained magnetite predominates.

The 30 samples in the microcline granite group GG7 exhibit paramagnetic properties, with a slight increase in remanence in some samples (Fig. 14). The one sample plotting in the 'magnetite' field differs from the normal microcline granites in having higher Sr, probably indicating a partly igneous source (Lahtinen 1996).

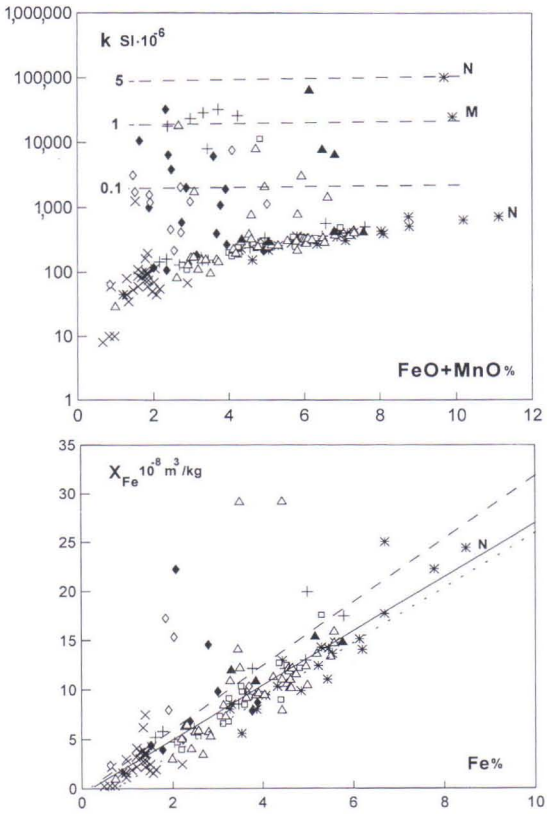

Fig. 13. Volume susceptibility (k) versus FeO+MnO diagram (upper figure) for granitoids in the Tampere–Hämeenlinna area, and mass susceptibility (X_{Fe}) versus Fe diagram (lower figure) for granitoids having k<1000 μSI. Data from this study. X_{Fe} is mass susceptibility minus the contribution from Mn, calculated by the formulas given in Puranen (1989). See Fig. 12 for symbols. The dashed lines with numbers in upper figure indicate the magnetite contents (wt%) calculated by formula given in Puranen (1989). Refer to Fig. 4 for lines in lower figure.

The GG8 granitoids occur mainly in the MB and very often have a sediment assimilated component, as seen in the occurrence of graphite in some samples (Lahtinen 1996). Three mafic samples are included in this group solely on the basis of high TiO_2 values, but otherwise they do not belong and are considered separately. In two of these, magnetite content is high (Fig. 14). The GG8 sample from the NTSB is a quartz monzodiorite and is geochemically comparable to differentiated K-rich high-Ti mafic plutonics with abundant magnetite, discussed in the mafic plutonic section. The sample from the MC is a quartz monzodiorite of 1812±2 Ma age (Vaasjoki 1995) with alkaline WPB affinity, having very high Ti, P, Sr, Ba, La and Zr (Lahtinen 1996). The remaining GG8 samples are from the MB and are paramagnetic, except for one sample with elevated susceptibilities that probably contains minute amounts of pyrrhotite (Fig. 14).

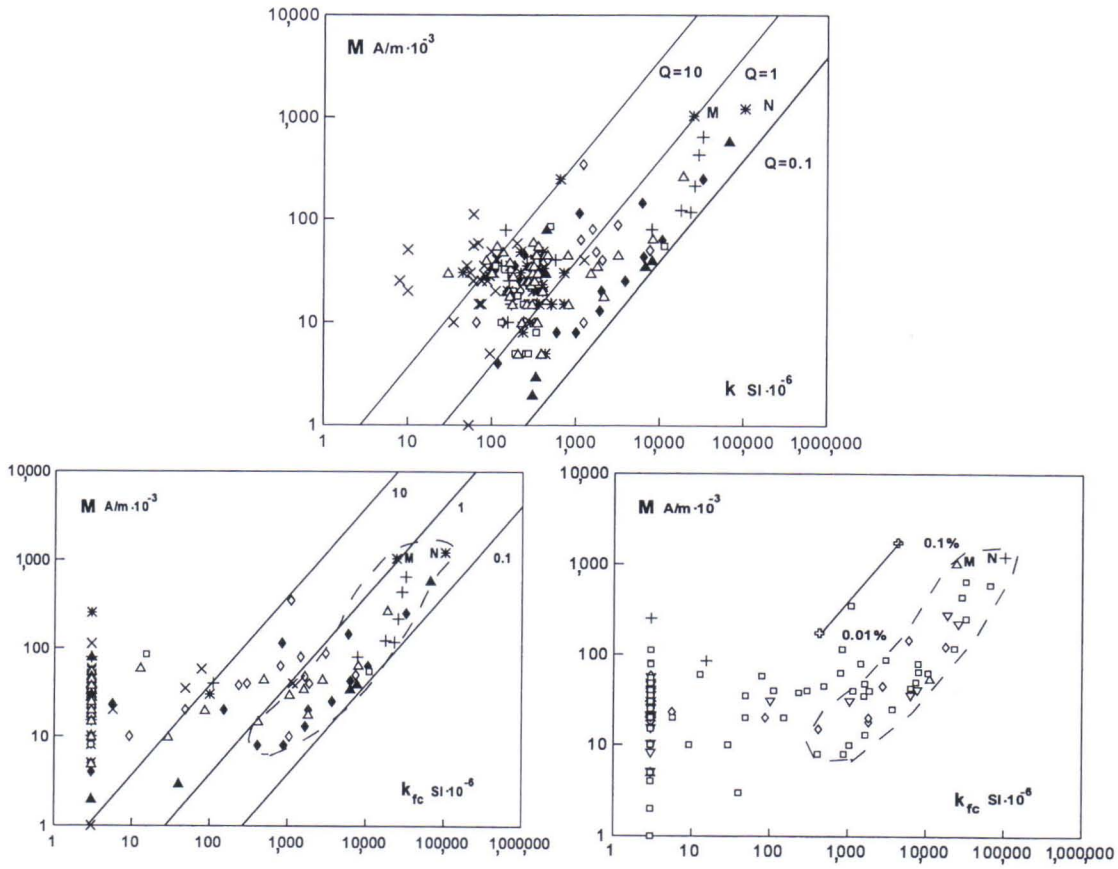

Fig. 14. Diagrams of intensity of NRM (M) versus volume susceptibility (k) (upper figure) and chemically estimated ferrimagnetic susceptibility diagrams (k_{fc}) (lower figures) for granitoids in the Tampere–Hämeenlinna area. Data from this study. See Fig. 13 for symbols in upper and middle figures. Q-ratios are indicated in upper figure and estimated Q_{fc}-ratios for ferrimagnetic susceptibilities are indicated in the lower left figure. The symbols in lower right figure are: open squares – samples <100 ppm S, open diamonds – 100–200 ppm S, open inverted triangles – 200–500 ppm S, open upright triangles – 500–1000 ppm S and crosses – >1000 ppm S. The line indicates the contribution from 0.01% to 0.1% sulphur calculated as pyrrhotite with susceptibility of 1,575,000 μSI and Q-ratio of 10. Lower figures: dashed line – 'magnetite' field.

Paramagnetic rocks

The paramagnetic nature of samples in this study was decided on the basis of chemical composition (Fe, Mn) and Curie's law (see p. 13). For comparison the paramagnetic and ferrimagnetic components (X_{pt} and X_{ft}) were then calculated physically for the 24 selected paramagnetic samples (using chemical criteria for preselection) by the method of Hrouda (1994, see p. 14). The results are displayed in Fig. 15, where X_{pt} and X_{ft} are shown versus total iron and versus the degree of oxidation. Almost every sample has a small ferrimagnetic component (average $2 \cdot 10^{-8}$ m^3/kg), indicating that pure paramagnetic rocks are rare or absent. Accordingly, NRM can be expected to occur in almost every rock type, at least in the sample set studied. X_{ft} values are slightly higher on average for felsic rocks (Fe 2–4%)

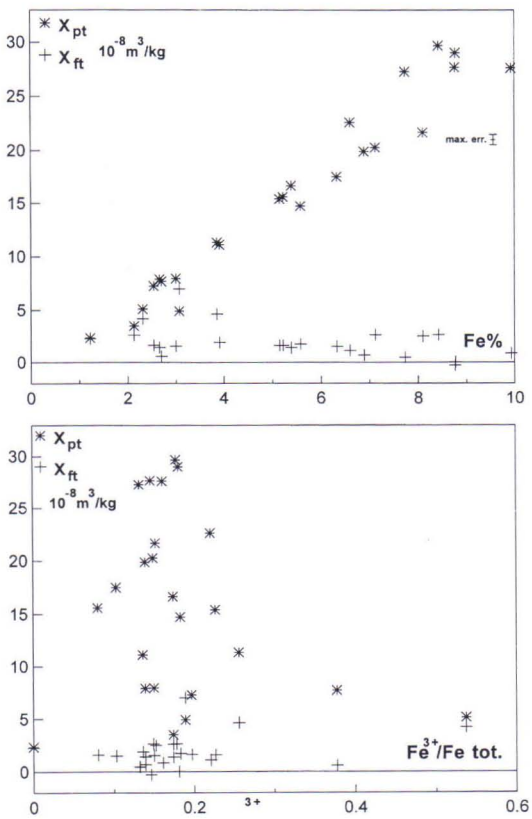

Fig. 15. Thermally estimated paramagnetic (X_{pt}) and calculated ferrimagnetic (X_{ft}) susceptibilities (method of Hrouda 1994, see p. 14) for set C samples versus total Fe (upper figure) and Fe^{3+}/Fe ratio (lower figure).

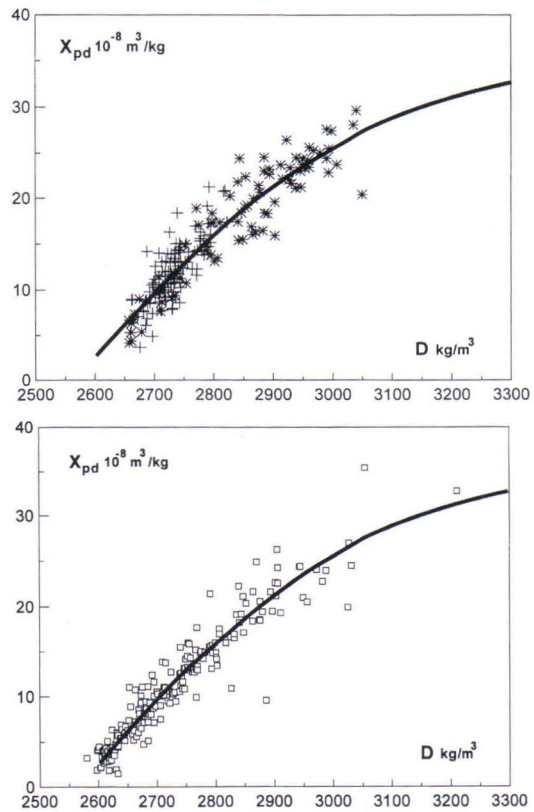

Fig. 16. Chemically estimated paramagnetic mass susceptibilities (calculated using Curie's law, p. 13) versus bulk density for sedimentary (crosses in upper figure), volcanic (asterisks in upper figure) and plutonic (open squares in lower figure) rocks in the Tampere–Hämeenlinna area. Also shown in both figures is the polynomial regression obtained using the data of this study. X_{pd} (estimated)(m^3/kg)=13.35+0.06161 x (d-2757.1)-0.00004789 x (d-2757.1)^2. R=0.90, Std (estimated)=2.06 m^3/kg

and possibly also for rocks having a higher degree of oxidation.

Chemical analyses are available for only a limited number of samples in the petrophysical register of the GSF and, thus, the paramagnetic component cannot be predicted in the normal way by applying Curie´s law. On the basis of the chemical and petrophysical data of this study we have evaluated the empirical relationship between paramagnetic susceptibility and bulk density. The estimated paramagnetic susceptibility was calculated from Fe and Mn data where the ratio of $Fe^{3+}/Fe_{tot.}$ was estimated to be 0.18 (see Fig. 15). Figure 16 shows the values of bulk density and paramagnetic susceptibility for the samples of this study and the polynomial regression calculated on the basis of these values. The regression equation is as follows:

$$X_{pd}\ (\text{estimated})(m^3/kg) = 13.35 + 0.06161 \times (d-2757.1) - 0.00004789 \times (d-2757.1)^2.$$

$$R = 0.90,\ \text{Std(estimated)} = 2.06\ m^3/kg$$

Although our data are somewhat scattered, this equation can be used as a first approximation of the level of the paramagnetic component in a sample where chemical determinations of Fe and Mn are not available. The equation appears to hold better for igneous rocks, while sedimentary rocks show a more inclined trend (Fig. 16).

Low–high susceptibility rock pairs

The GSF petrophysical register contained measured values of density, volume susceptibility and intensity of NRM for most of the 130,756 samples included at the end of 1996. In the Tampere–Hämeenlinna area, systematic sampling has been done from map sheets 2113 and 2124, with three or more samples taken by hammer from individual outcrops. The samples were selected by magnetometer and susceptimeter to represent the different magnetic populations, if variation existed. For purposes of the present study, 36 outcrops were selected and two samples of the same rock type were analysed from each. Some of these sample pairs were selected on the basis of great difference in susceptibility values, as this would indicate the occurrence of a paramagnetic–ferrimagnetic pair in the same rock types. Polished thin section studies were made on all samples to determine the amounts of ferrimagnetic minerals and sulphides (Pennanen 1991). The petrophysical properties and opaque mineralogy of 20 sample pairs are set out in Table 2 along with the calculated values of k_{fc} and Q_{fc}.

According to Pennanen (1991), many of the above samples contain martite, and locally hematite occurs as a magnetite pseudomorph. Sphene frequently occurs as a reaction rim between ilmenite and silicate minerals. Similar rims have been observed for magnetite and hematite. Ilmenite exsolutions in magnetite, and magnetite exsolutions in ilmenite, also have been observed and have been interpreted to originate from oxidation of ulvite to ilmenite (Pennanen 1991). These titanomagnetites may lose their magnetite component through dissolution in hydrothermal fluids or weathering solutions, so that only the ilmenite skeleton is left behind. Ilmenite-hematite exsolution structures are found in a few samples. Chalcopyrite and pyrite often have an alteration rim of iron hydroxides indicating the effect of weathering solutions.

Although the samples in Table 2 were selected to represent paramagnetic–ferrimagnetic pairs, in many cases the presumed paramagnetic sample has a small ferrimagnetic component. Sample pairs 3–5, 7–10 and 20 are granitoids with similar chemistry and the two samples of these pairs can thus be considered to represent one and the same magma.

Table 2. Density (D), susceptibility (k), intensity of NMR (M), estimated ferrimagnetic susceptibility (k_{fc}) and estimated ferrimagnetic Q_{fc}-ratio ($M/(0.041 x k_{fc})$) for selected (set B) low and high susceptibility pairs (from same outcrop) from the study area, taken from the GSF petrophysical register. Opaque mineralogy (Pennanen 1991). Ferrimagnetic susceptibility is the measured susceptibility minus paramagnetic susceptibility calculated using Curie's law assuming that all Fe is present as Fe^{3+}.

P[1]	Rock type	D kg/m^3	k SI·10^{-6}	M A/m·10^{-3}	k_{fc} SI·10^{-6}	Q_{fc}	Opaques[2]
1	Granodiorite	2705	350	10	80	3.1	(ILME)
1	Quartz diorite	2785	11,900	70	11,400	0.15	MAGN,ILME,PYR,CHAL
2	Volcanic rock	2799	490	10	0	-	PYR,CHAL,ILME
2	Volcanic rock	2787	64,740	350	64,080	0.13	MAGN,HEMA
3	Tonalite	2790	890	10	420	0.58	PYR,ILME,MAGN
3	Quartz diorite	2777	4,050	40	3,520	0.28	MAGN,PYR,ILME,MART
4	Granodiorite	2644	410	20	190	2.6	(PYR,ILME,MAGN?)
4	Granodiorite	2664	1,700	30	1,500	0.49	ILME,MAGN,PYR,CHAL
5	Granite	2678	1,920	30	1,640	0.45	MAGN,MART
5	Granite	2688	13,680	200	13,440	0.36	MAGN,PYR,CHAL,ILME
6	Granodiorite	2645	80	0	0	-	-
6	Granite	2662	1,780	20	1,540	0.32	MAGN,MART,ILME
7	Granite	2596	260	10	160	1.5	(MAGN,MART)
7	Granodiorite	2628	2,060	20	1,920	0.25	MAGN,MART
8	Granite	2550	260	0	140	-	(MART,MAGN,ILME,PYR)
8	Granite	2530	7,630	140	7,480	0.46	MAGN,MART
9	Granite	2575	450	20	350	1.4	(MAGN,MART)
9	Granite	2520	2,110	50	2,030	0.60	MAGN,MART
10	Granite	2560	840	10	630	0.39	MART,MAGN
10	Granodiorite	2650	2,060	20	1,860	0.26	MAGN,MART
11	Volcanic rock	2961	740	20	0	-	-
11	Volcanic rock	3197	4,210	70	3,060	0.56	PYR,CHAL
12	Hornblendite	2996	790	30	0	-	(PYRR,ILME)
12	Hornblendite	3069	25,280	1,670	24,250	1.7	PYRR,ILME,MAGN,CHAL
13	Volcanic rock	2713	410	490	100	100	HEMA,(MART?)
13	Volcanic rock	2714	2,260	410	1,940	5.2	MART,HEMA,MAGN
14	Volcanic rock	2847	600	10	140	1.7	ILME,MAGN,PYR,MART
14	Volcanic rock	2956	2,670	50	2,060	0.59	MAGN,CHAL,PYR,ILME
15	Volcanic rock	2895	590	10	0	-	(ILME)
15	Volcanic rock	3020	3,150	30	2,160	0.34	MAGN,MART
16	Volcanic rock	2738	420	10	0	-	(ILME)
16	Volcanic rock	2884	4,170	3,660	3,670	24.3	PYRR,CHAL,ILME
17	Diorite	2838	830	10	140	1.7	ILME,MAGN,MART,PYRR
17	Diorite	2865	7,770	60	7,030	0.21	ILME,PYR,MAGN,CHAL
18	Quartz diorite	2762	2,140	30	1,660	0.44	PYR,ILME,MAGN
18	Quartz diorite	2752	59,160	360	58,440	0.15	MAGN,PYR,CHAL,ILME
19	Volcanic rock	2777	550	10	0	-	ILME,PYR,CHAL
19	Volcanic rock	2749	5,380	50	4,880	0.25	ILME,PYR,CHAL
20	Granodiorite	2550	660	20	470	1.0	(MAGN,PYR,ILME)
20	Granodiorite	2608	2,790	20	2,610	0.19	MAGN,MART,PYR,ILME

[1] Sample pairs 1–11 from Viljakkala–Teisko area and 12–20 from Forssa area.
[2] Ferrimagnetic opaques and sulphides. Parentheses indicate minute amount of opaques. MAGN – magnetite, MART – martite, ILME – ilmeniitti, HEMA – hematite, PYR – pyrite, PYRR – pyrrhotite, CHAL – chalcopyrite.

All these samples contain magnetite, ilmenite and martite as ferrimagnetic minerals. The observed differences in k_{fc} are evidently due to the heterogeneous occurrence of magnetite and to a lesser extent also of ilmenite in the samples, combined with the dissimilar amounts of martite.

The pair 1 samples clearly represent two different rock types as seen in the SiO_2 65.4–55.0%, Zr 152–351 ppm, Nb 5.6–15.1 ppm, Ba 946–1460 ppm and La 19.5–40.4 ppm (granodiorite–quartz diorite, respectively). The granodiorite belongs to the high-K calc-alkaline group (GG2) normally characterized by paramagnetic properties (see above). The quartz diorite has indications of hybrid origin with large high-Ti WPB component, and the occurrence of magnetite may be explained by hybrid origin. The paramagnetic granodiorite of pair 6 also has geochemical characteristics comparable with the normally paramagnetic high-K calc-alkaline group. The ferrimagnetic granite sharply differs from the granodiorite in belonging to the normally ferrimagnetic very high-K group of tholeiitic affinity (GG6).

The diorite samples of pair 17 are geochemically similar and the difference in K_{fc} values is probably due to the heterogeneous occurrence of ferrimagnetic minerals. The sample with lower susceptibility in the quartz diorite pair 18 is a hybrid rock, as seen in small mafic enclaves. Both samples contain magnetite and ilmenite (Table 2). The quartz diorite with higher susceptibility differs from its pair in containing more Al_2O_3 (19.8–16.6%), FeO (10.5–6.8%), P_2O_5 (0.64–0.21%), S (2610–108 ppm), Sr (604–397 ppm), Zr (276–132 ppm) and Ba (416–187 ppm), but also lower V (77–211 ppm) and Sc (12.7–26). The magnetite in the sample is anhedral and could indicate nonmagmatic origin in pyrite mineralization (high S).

The paramagnetic sample of volcanic pair 2 contains about 25% carbonate with elevated contents of some sulphur-related elements, indicating mineralization effects. The ferrimagnetic volcanic rock contains, in addition to magnetite, also hematite that is not martite (Table 2). The mafic volcanic pair 11 is from the Haveri Formation (Kähkönen 1989) and there is no mineralogical explanation for the higher susceptibility of one of the samples. Compared with the paramagnetic hornblendite, the olivine hornblendite of pair 12, containing both pyrrhotite and magnetite, has geochemical indications of a more cumulated and mineralized nature.

The samples of the volcanic rock pair 13 are chemically similar and the difference in susceptibility can be attributed to the uneven distribution of magnetite and the greater amount of hematite/martite in the sample with lower susceptibilities. The same situation holds for pair 14. The magnetite-bearing mafic volcanic rock of pair 15 has higher FeO (13.0–9.3%) and CaO (14.0–9.7%), lower SiO_2 (44.5–51.3%) and Na_2O (1.7–3.7%) and slightly higher La (12.3–7.7 ppm) and Cu (49–18 ppm). The strong alteration of the sample, as seen in the abundance of epidote and zoisite (about 40%), is responsible, at least in part, for this geochemical composition. Magnetite occurs as euhedral and partly corroded crystals with some martite. The formation of magnetite could be connected with alteration.

The occurrence of pyrrhotite explains the higher susceptibility of one of the samples of volcanic pair 16, but there is no evident mineralogical explanation of the higher susceptibility of one sample of pair 19. The low S (55 ppm) relative to the low Q-ratio suggests a small amount of magnetite occurring very heterogeneously.

AREAL CORRELATIONS BETWEEN POTENTIAL FIELDS AND PETROPHYSICAL PROPERTIES

Characteristic statistical parameters of bulk density, volume susceptibility and intensity of NRM calculated for the different rock types and groups and the five main geological divisions of this study are set out in Table 3. The total magnetization and density of samples are shown in two projected profiles in Fig. 17, and an aeromagnetic anomaly map and a pair of regional residual separation maps are shown in Fig. 2a and 2b. The average density variation of profiles corresponds in a general way with the mean Bouguer anomalies (Fig. 1b). The area of higher density in the HSB in the western profile, and the negative anomaly coinciding with microcline granites from the MC in the eastern profile, are also seen as positive and negative regional anomalies, respectively, in Fig. 1b. The higher average density in the HSB is due to the abundant occurrence of tholeiitic mafic volcanic and plutonic rocks (Table 3). There is a slight decrease in average density from the southern part of the MB towards the north. This is due to the occurrence of volcanics (VG1 in Table 3) and to the higher proportion of mafic plutonics in the south. The slight increase in density in the NTSB, apparent in the eastern profile, is due to the HiSB and some mafic plutonic rocks.

The averages of bulk density, magnetization, magnetic DGRF-65 anomaly and Bouguer anomaly were calculated for 20x20 km cells (Fig. 18 and Table 4). A modified Bouguer anomaly was calculated as well, to reduce the effect of the long wavelength Bouguer anomaly component. The long wavelength Bouguer anomaly component displays a strong negative correlation with land uplift values (Elo 1992). This long wavelength trend was fitted, by least squares, to 50x50 km averages of Bouguer anomalies for southern and central Finland, and the 1st order trend surface that was obtained was subtracted from the 20x20 km cell results (Table 4).

Average DGRF-65 anomalies versus average magnetizations are shown in Fig. 19, and average values of the original and modified Bouguer anomalies versus average bulk densities are shown in Fig. 20. The average level of the magnetic field varies from -250 to +400 nT, and the modified Bouguer anomaly varies from -1 to +17 mGal. A comparison of these values with the petrophysical properties of the surface bedrock shows the deep magnetic anomaly component to range at least from -250 (shallow formations) to +50 nT (deep formations) and reversing the depth ratios perhaps from -600 to +400 nT. The deep model was calculated by using a magnetized half space of H=41 A/m and I=75°. The shallow model was a thin horizontal layer. Low average Q-values (Q<1.5) correspond to variable and mainly positive DGRF-65 anomaly averages. High Q-values are variable and correspond to smooth and always negative anomaly averages.

The deep magnetic anomaly component in the MC varies between 0 and 400 nT (Fig. 19) depending on the thickness of the surface formations. The MC is characterized by low density rocks at surface level. The high, almost constant, base level of 16 mGal indicates the occurrence of hidden mass correlating with the relatively high regional deep magnetic anomaly level (+80 nT), determined from the two MC cells.

The deep anomaly component in the HSB may range from -600 to 0 nT. If the component is constant, the value is -200 nT. The layer for surficial magnetization may be shallow in some cells and relatively deep in others. The poor correlation between average DGRF-65 anomalies and average magnetizations of apparently shallow sources may be due to change in the direction of the intensity of NRM (partly pyrrhotite) hampering the interpretation. A notable feature is that the cells (HSB/4–6) for which shallow depth is

Table 3. Arithmetic mean of density (D), volume susceptibility (k), intensity of NMR (M) and Q-ratio for all samples and for subareas (Fig. 2), rock types and selected groups within them. D_{pp}, k_{pp}, M_{pp} and Q_{pp} , and D_{fp}, k_{fp}, M_{fp} and Q_{fp} are means for paramagnetic and ferrimagnetic populations defined as $k_{fc} \leq k_{pc}$ and $k_{fc} > k_{pc}$, respectively. K_{pc} is paramagnetic susceptibility calculated using Curie's law assuming that all Fe is present as Fe^{3+} and $k_{fc} = k - k_{pc}$. The proportion of samples having $k_{fc} > 0$ (F1), $k_{fc} > k_{pc}$(F2), $J > 0.25$ A/m (F3) and $J > 2.5$ A/m (F4) and the number of samples having predicted magnetite (Mt), predicted pyrrhotite (Pyrr) or minute amounts of ferrimagnetic material (Others) are indicated. F3 and F4 cause 50 nT and 500 nT anomalies, respectively, for a sheet-like body.

	N	D	D_{pp}	D_{fp}	k	k_{pp}	k_{fp}	M	M_{pp}	M_{fp}
			kg/m^3			$SI \cdot 10^{-6}$			$A/m \cdot 10^{-3}$	
Total	403	2656.4	2756.0	2757.6	3,907	359	16,790	182	78	560
NTSB	67	2734.8	2771.0	2705.4	6,631	389	11,691	165	28	277
TSB	58	2730.9	2729.1	2740.6	3,737	305	22,426	62	36	205
MB	140	2744.2	2741.1	2814.2	470	311	4,019	159	40	2,826
HSB	107	2825.1	2818.8	2848.2	5,169	513	22,172	295	193	666
MC	31	2668.8	2630.6	2729.3	9,499	113	24,360	162	34	364
Sedimentary rocks	112	2733.1	2732.3	2741.6	1,485	296	13,616	300	115	2,177
SG1	17	2721.4	2727.6	2692.3	3,404	266	18,048	336	31	1,756
SG3	18	2704.7	2704.7	-	198	198	-	25	25	-
SG4	28	2719.3	2719.3	-	254	254	-	53	53	-
SG5	15	2738.0	2734.7	2784.0	504	300	3,363	654	545	2,184
SG6	10	2770.3	2770.3	-	461	461	-	107	107	-
SG7	7	2753.3	2753.3	-	405	405	-	49	49	-
SG7/MC	4	2752.3	2762.0	2742.5	15,207	408	30,007	232	38	423
Black schists	4	2747.0	2708.0	2760.0	3,578	195	4,706	2,613	20	3,477
Volcanic rocks	84	2848.9	2863.0	2822.1	9,131	618	25,278	236	136	426
VG1	5	2965.0	2965.0	-	901	901	-	98	98	-
VG2	9	2918.0	2933.3	2887.3	1,434	836	2,887	108	62	202
VG3	24	2928.1	2937.9	2911.7	10,882	771	27,735	275	60	632
VG4	3	2891.3	2891.3	-	594	594	-	35	35	-
VG5	18	2824.4	2847.0	2789.0	17,492	581	44,068	480	440	544
VG6	19	2729.2	2709.5	2756.3	7,311	268	16,995	93	50	152
VG7	4	2782.8	2865.0	2700.5	8,044	358	15,555	290	64	515
Mafic plutonics	35	2910.5	2906.2	2927.4	3,663	647	15,727	276	62	1,137
NTSB+TSB	11	2899.4	2906.0	2869.5	5,231	644	25,871	70	32	244
MB	7	2920.1	2901.7	3031.0	795	576	2,108	249	72	1,308
HSB	17	2913.6	2908.5	2930.5	3,831	683	14,061	442	78	1,540
Granitoids	172	2695.0	2697.6	2686.8	2,981	238	11,744	61	29	162
GG1	7	2780.6	2764.5	2802.0	11,817	379	27,067	111	29	222
GG2	45	2718.5	2718.8	2716.9	1,045	263	4,660	35	28	65
GG3	16	2708.4	2706.4	2739.0	951	260	11,325	25	23	55
GG4	19	2711.9	2725.6	2682.3	7,362	273	22,723	105	29	270
GG5	13	2644.0	2661.3	2638.8	1,622	190	2,051	67	23	81
GG6/NTSB	13	2650.9	2660.3	2646.8	4,330	223	6,155	54	20	70
GG6/Others	5	2650.4	2656.8	2625.0	2,280	194	10,625	36	29	63
GG7/MC	21	2616.8	2617.1	2611.0	130	75	1,250	33	32	40
GG7/Others	9	2618.6	2618.6	-	74	74	-	34	34	-
GG8/(MB+HSB)	21	2744.4	2744.4	-	352	352	-	35	35	-

Table 3 (continued).

	N	Q	Q_{pp}	Q_{fp}	F1 %	F2 %	F3 %	F4 %	Mt	Pyrr	Others
Total	403	5.9	6.7	2.8	33	22	16	4	72	27	32
NTSB	67	1.5	2.4	0.8	70	55	27	3	32	0	15
TSB	58	4.1	4.5	1.9	26	16	12	2	9	2	4
MB	140	4.8	4.3	15.9	12	4	6	2	0	11	3
HSB	107	9.4	10.9	4.0	37	21	20	7	20	13	6
MC	31	11.2	17.7	0.9	48	39	32	6	10	1	3
Sedimentary rocks	112	9.0	9.0	8.7	17	9	10	5	5	9	5
SG1	17	3.3	3.5	2.1	24	18	12	6	3	0	1
SG3	18	3.5	3.5	-	0	0	0	0	0	0	0
SG4	28	5.1	5.1	-	0	0	0	0	0	0	0
SG5	15	39.9	41.6	15.8	13	7	13	7	0	1	1
SG6	10	3.6	3.6	-	20	0	0	0	0	2	0
SG7	7	2.7	2.7	-	43	0	0	0	0	2	1
SG7/MC	4	1.4	2.2	0.5	50	50	50	25	2	0	0
Black schists	4	12.6	2.5	16.0	75	75	75	50	0	3	0
Volcanic rocks	84	4.5	5.0	3.6	51	35	31	8	25	12	6
VG1	5	2.5	2.5	-	40	0	20	0	0	2	0
VG2	9	1.9	1.8	2.1	56	33	11	0	2	2	1
VG3	24	2.2	1.7	3.0	54	38	33	13	7	5	1
VG4	3	1.4	1.4	-	0	0	0	0	0	0	0
VG5	18	10.4	12.1	7.7	56	39	44	22	6	3	1
VG6	19	4.2	6.9	0.6	47	42	32	0	8	0	1
VG7	4	4.9	3.1	6.6	75	50	50	0	1	0	2
Mafic plutonics	35	2.6	2.4	3.3	40	20	20	3	8	6	0
NTSB+TSB	11	1.1	1.3	0.2	36	18	18	0	3	1	0
MB	7	5.1	3.5	15.1	29	14	14	0	0	2	0
HSB	17	2.5	2.6	1.9	47	24	24	6	5	3	0
Granitoids	172	5.1	6.5	0.7	32	24	12	1	34	0	21
GG1	7	1.0	1.6	0.2	57	43	43	15	3	0	1
GG2	45	3.1	3.7	0.5	24	18	4	0	7	0	1
GG3	16	2.1	2.3	0.1	13	6	6	0	1	0	1
GG4	19	2.4	3.4	0.3	37	32	32	0	6	0	1
GG5	13	2.0	3.1	1.6	92	77	15	0	5	0	7
GG6/NTSB	13	1.2	2.8	0.5	85	69	23	0	9	0	2
GG6/Others	5	2.8	3.5	0.1	20	20	20	0	0	0	1
GG7/MC	21	17.6	18.5	0.8	14	5	0	0	1	0	2
GG7/Others	9	18.7	18.7	-	0	0	0	0	0	0	1
GG8/(MB+HSB)	21	2.9	2.9	-	5	0	5	0	0	0	1

indicated are ones occurring adjacent to the MB and partly overlapping it. Good correlation between bulk density and modified Bouguer anomaly exists in the HSB (Fig. 20). An interpretation based on both magnetic and gravity data indicates that the HSB is a moderately deep formation and part of the area may be underlain by a deep magnetic source.

The deep magnetic anomaly component in the MB may vary from -550 to -200 nT (Fig. 18) and expressed at constant level is -250 nT. The poor correlation between average DGRF-65 anomalies and average magnetizations may be due to change in the direction of the intensity of the NRM (partly pyrrhotite), which reduces the average magnetization. The high magnetic base levels to the south (MC) and north (NTSB, see below) of the MB indicate that the MB must be a thick formation to account for so large a contrast in the regional anomaly. There is only a small variation in both bulk density and gravity in the MB and no clear correlation between the two exists. The modified Bouguer anomaly varies from 8 to 13 mGal at similar bulk densities indicating the occurrence of locally hidden masses. Together these findings suggest a variable but considerable base thickness for the MB, and

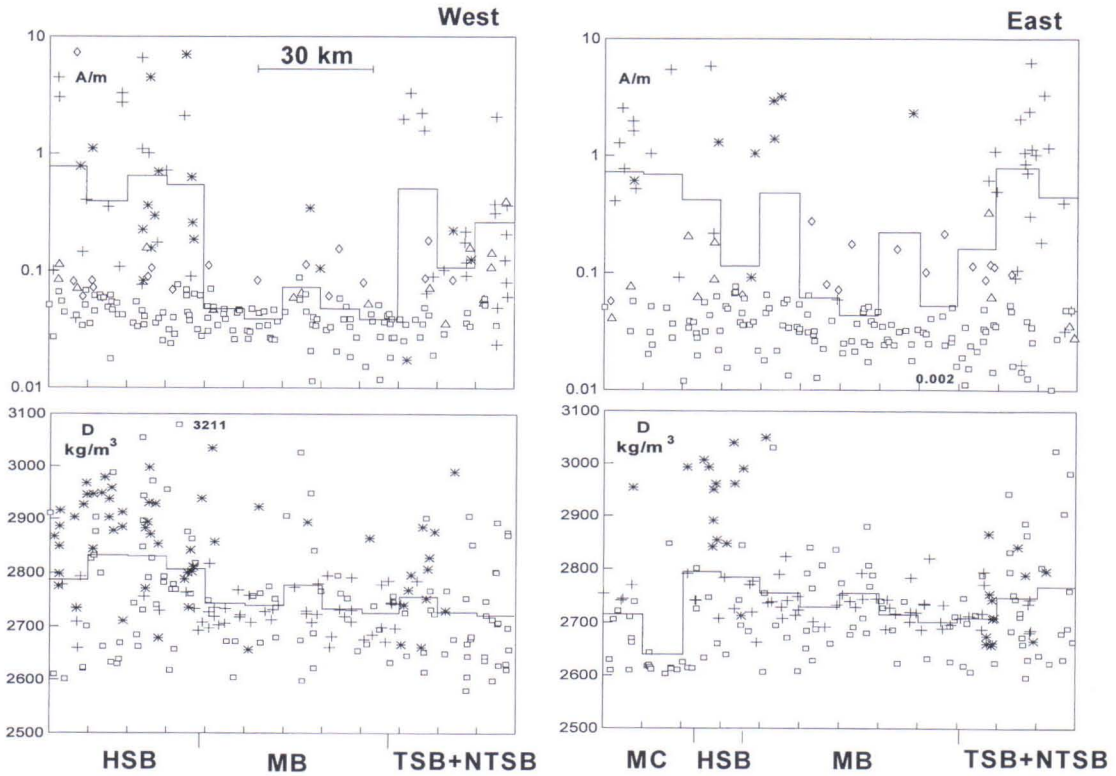

Fig. 17. Total magnetization (upper figure) and bulk density (lower figure) of samples in the study area. The study area has been divided into two equal-sized subareas 40x120 km (west–east), and the samples are projected onto two N–S lines. Symbols in upper figures: open squares – paramagnetic samples with intensity of NRM $\leq 50 \cdot 10^{-3}$ A/m, open diamonds – paramagnetic samples with intensity of NRM $>50 \cdot 10^{-3}$ A/m, open triangles – samples interpreted to contain mainly hematite (martite), crosses – samples interpreted to contain mainly magnetite and asterisks – samples interpreted to contain mainly pyrrhotite. Symbols in lower figures: crosses – sedimentary rocks, asterisks – volcanic rocks and open squares – plutonic rocks. Solid lines – the average of samples calculated every 10 km. The approximate areal boundaries are shown below (see Fig. 2). MC – Microcline granite Complex, HSB – Hämeenlinna Schist Belt, MB – Mica gneiss–migmatite Belt, TSB – Tampere Schist Belt, NTSB – North of TSB.

the average vectorial magnetization is probably smaller than the apparent average magnetization calculated from scalar magnetization intensities of rock samples.

The TSB exhibits a deep magnetic anomaly component between about -250 and 0 nT. In regional anomalies the sources are likely to be shallow with a variation of -150 to 0 nT. The lack of correlation between the average DGRF-65 anomalies and average magnetizations indicates that the variation in the magnetic field is mainly due to deep sources. No correlation exists between bulk density and gravity, and the mean gravity anomaly is constant, implying either mass equilibrium between blocks or further that the TSB surface formations are shallow. A combined analysis of the magnetic field and gravity data confirms that the TSB is a shallow formation, where the deep magnetic anomaly varies, while the bulk density difference and thickness or their product are more or less constant for different cells. The TSB forms a boundary zone between the MB and NTSB and the calculated TSB cells extend into the MB and NTSB (Fig. 18). The difference between the western (higher J and lower DGRF-65 anomaly) and eastern (lower J and higher DGRF-65 anomaly) parts of the TSB could be interpreted to indicate that the cover over the deep anomaly is shallower in the east than in the west.

The deep magnetic anomaly component in the NTSB may range from -100 to +350 nT and expressed as a constant value is +100 nT. This is comparable to the value for the MC. Poor correlation exists between bulk density and the modified Bouguer anomaly, and the modified Bouguer anomaly level is low (about 0 mGal). This could mean that surface rocks occur as a thin layer and that there is a deep source of low density rocks. Interpretation of the magnetic and gravity data together indicates that the surface formations in the NTSB are rather shallow and underlain by a low density deep source with variable magnetizations.

The smoothed map in Fig. 2b shows mainly regional features of magnetization, which at least in part are due to a deeper source, as discussed above. The sharper thin anomalies (derived map in Fig. 2b) are due to magnetic rocks at the present erosion level. The TSB can be divided into two parts: a southern part with abundant sediments and plutons characterized by a highly negative magnetic low comparable to the MB and a northern volcanic part showing a higher magnetic field. These same features are seen in the two profiles of Fig. 17 where the MB shows very low values

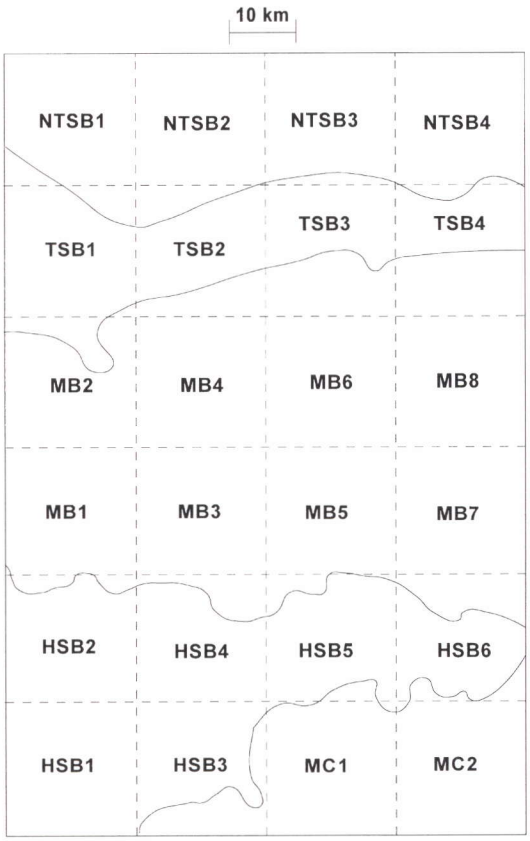

Fig. 18. Division of the study area into 20x20 km cells used as basis for the calculations of parameters in Table 4. Cells are overlain on the geological subunits used in this study (see Fig. 2). MC – Microcline granite Complex, HSB – Hämeenlinna Schist Belt, MB – Mica gneiss–migmatite Belt, TSB – Tampere Schist Belt, NTSB – North of TSB.

Table 4. Areal means of density (D), volume susceptibility (k), intensity of NMR (M) and total magnetization (J) calculated in 20x20 km cells (Fig. 18) using the data of this study weighted by the areal-% of main rock types (granitoids, mafic plutonics, sedimentary rocks and volcanic rocks) in each cell. Q-ratio is calculated from areal means of k and M (Q=M/(0.0041xk)). Also included are the areal means of magnetic DGRF-65 anomalies (F), Bouguer anomalies ($\triangle G_B$) and regional Bouguer anomalies ($\triangle G_{BC}$) corrected for long wavelength for same cells.

Area	D kg/m^3	k SI·10^{-6}	M A/m·10^3	J mA/m	Q-ratio	F nT	$\triangle G_B$ mGal	$\triangle G_{BC}$[1] mGal
MC1	2704	23,471	315	1,278	0.33	409.2	-0.5	15.4
MC2	2653	3,209	88	219	0.67	130.3	2.1	16.7
HSB1	2777	6,526	120	387	0.45	23.7	-10.0	8.5
HSB2	2749	1,460	204	263	3.4	-51.5	-13.3	5.7
HSB3	2772	3,782	185	340	1.2	-21.5	-2.9	14.3
HSB4	2805	2,528	698	802	6.7	-126.5	-3.7	14.0
HSB5	2804	6,930	105	388	0.37	-146.9	-2.8	13.6
HSB6	2754	386	164	180	10.4	-181.0	-8.6	6.6
MB1	2723	275	40	52	3.6	-238.1	-9.4	10.2
MB2	2732	294	38	51	3.2	-216.8	-11.6	8.5
MB3	2745	470	49	68	2.5	-246.6	-6.9	11.4
MB4	2743	332	47	61	3.5	-223.3	-8.8	10.0
MB5	2744	346	88	101	6.2	-170.2	-3.6	13.4
MB6	2716	274	17	28	1.5	-186.9	-3.8	13.8
MB7	2734	946	514	553	13.3	-207.0	-3.8	11.9
MB8	2743	524	206	228	9.6	-200.7	-3.6	12.7
TSB1	2720	3,265	53	187	0.40	-117.9	-16.9	3.8
TSB2	2735	5,429	66	289	0.30	-61.1	-15.0	4.4
TSB3	2719	1,086	57	101	1.3	-32.2	-14.1	4.0
TSB4	2707	1,132	30	76	0.65	16.5	-11.9	4.9
NTSB1	2688	1,794	66	140	0.90	114.9	-21.8	-0.6
NTSB2	2738	3,419	108	249	0.77	195.2	-20.6	-0.5
NTSB3	2715	5,156	278	489	1.3	176.6	-19.4	-0.7
NTSB4	2731	12,898	154	682	0.29	351.1	-16.6	0.9

[1] The regional long wavelength trend of first order was calculated using 50x50 km cells and used to subtract the transient mantle effects from the measured Bouguer anomalies: $\triangle G_{BC} = \triangle G_B + 18.81 + 0.0280(x-6740) - 0.0642(y-460)$, where grid coordinates x= 6740 and y= 460 define the SW corner of the study area.

of average magnetization with a few higher peaks due to the occurrence of pyrrhotite-bearing rocks. The low areal Q-ratios for the MC, TSB and NTSB show the predominance of magnetic susceptibility in the magnetization (Table 4). This is in agreement with the predicted occurrence of magnetite and lack of pyrrhotite in these areas (Table 3). Intensity of NRM predominates in the magnetization in the MB, and there are no samples with predicted magnetite. In its samples bearing both magnetite and pyrrhotite, the HSB has characteristics intermediate between the MC, TSB and NTSB on the one hand and the MB on the other (Table 3).

Magnetic anomalies in the NTSB, TSB, HSB and MC are partly due to magnetite±hematite-bearing granitoids (excluding microcline granites), mafic plutonic rocks, volcanic rocks and in the NTSB (HiSB) and the MC also to magnetite-bearing sedimentary rocks (Table 3). The strong magnetic anomalies in the NTSB are probably due to volcanic and sedimentary rocks like those found in the HiSB, but also one GG1 granitoid and one high-Ti mafic granitoid exhibit high magnetic susceptibility. The intermediate to strong magnetic anomalies in the TSB are due to VG5–VG7 volcanic rocks, where evidently the strongest magnetic anomalies occur in the VG5 rocks. The Upper Volcanic Unit at Ylöjärvi (Kähkönen 1989) was not sampled in this study, but the aeromagnetic map shows it to be strongly magnetic. This is confirmed in the abundant occurrence of magnetite in this unit (ibid.). The strong magnetic anomalies in

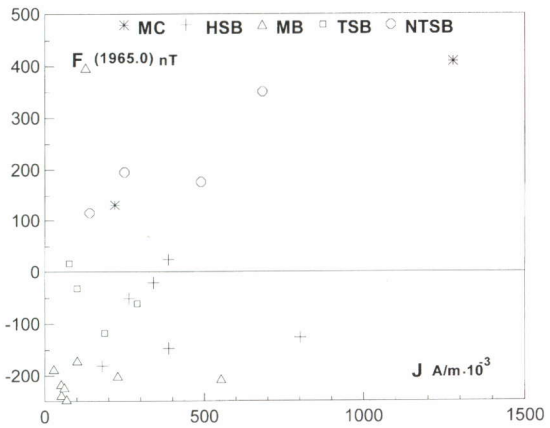

Fig. 19. Averages of magnetic DGRF-65 anomalies versus magnetization (J) in the Tampere–Hämeenlinna area calculated in 20x20 km cells. Refer to Figure 18 and Table 4.

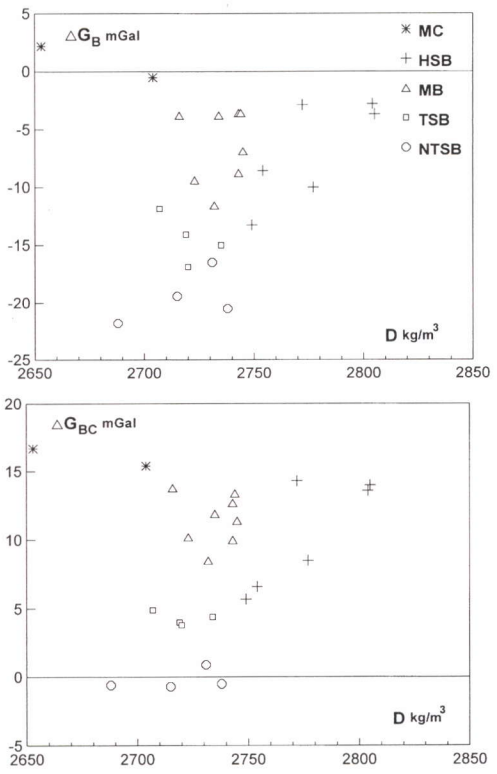

Fig. 20. The average Bouguer anomalies (upper) and average long wavelength suppressed (lower) Bouguer anomalies versus average bulk densities in the Tampere–Hämeenlinna area calculated in 20x20 km cells. Refer to Figure 18 and Table 4.

the HSB are mainly due to tholeiitic group VG3 volcanic rocks, especially the trachytic variants, but also some VG5 volcanic rocks and tholeiitic mafic plutonics show strong magnetic anomalies. Many of the irregularly shaped strong magnetic anomalies in the MC are explained by magnetite-bearing migmatites, while the more regular anomalies may indicate the occurrence of magnetite-bearing WP-originated plutons.

The strong local anomalies in the MB are due to the pyrrhotite-bearing black schists and SG5 sediments. The granitoids, mafic plutonic rocks and volcanic rocks in the area belong mainly to the paramagnetic population. Although the occurrence of magnetite cannot be totally excluded, the data of this study indicate that pyrrhotite is the main source of the strong local magnetic anomalies in the MB. In addition to the ferrimagnetic samples, some of the samples belonging to the paramagnetic population have high values of intensity of NRM, possibly producing local anomalies. The magnetization of samples of this study is plotted on the derived map of Fig. 2b, which was processed to visualize sharp magnetic anomalies. On the whole, the correlation between magnetization of samples and shallow magnetic anomalies is good; exceptionally magnetic anomalies are numerous in the northern part of the MB but only one sample exhibits high magnetization. The anomalies are probably due to the abundant occurrence of pyrrhotite-bearing black schists in the area, which were not sampled in this study.

DISCUSSION

The bulk density of the different rock types for the most part is correlated with the abundances of ferromagnesian minerals and K-feldspar, the first increasing the density and the latter decreasing it. Within granitoids there is a trend from the denser hornblende-dominated mafic samples via biotite-dominated intermediate samples to felsic K-feldspar-dominated samples. Normally the amount of quartz and the albite component in plagioclase increase towards the felsic samples. The effect of more anorthite-rich plagioclase or less K-feldspar in samples of lower K is seen as a deviation to higher densities. This general 'differentiation' trend holds not only for granitoids but for mafic plutonic rocks and to some extent also for volcanic rocks of the study area, though the tholeiitic volcanics tend to have more iron-rich ferromagnesian minerals, which increase the density at similar FeO+MnO+MgO values. The situation for the sedimentary rocks is more complex due to the more variable mineralogy. Although the same general trend is observed, from higher densities in more mafic samples to lower densities in felsic samples, the variation is much wider. The occurrence of muscovite, andalusite, sillimanite, garnet and/or sulphides increases the density relative to biotite-dominated samples, whereas metamorphic K-feldspar and/or cordierite lower the density of some garnet±sillimanite-bearing samples.

As seen in the SG5 group sedimentary rocks, black schists and mafic plutonics of the MB, samples that contain pyrrhotite are of higher density. In general, the magnetite-bearing volcanic rocks and granitoids of the ferrimagnetic population are lower in density than similar rocks of the paramagnetic population. This is seen especially clearly in the tholeiitic VG3 volcanics from the HSB. Our explanation for the lower density and crystallization of magnetite (see below) in some volcanics is the more fluid enriched and differentiated nature of magmas, which due to escape of a fluid phase during extrusion more

easily form volcanic breccias and hydrostatically fractured parts of pyroclastic flows. The lower density for magnetite-bearing samples is probably due to the more hydrated state of the minerals; the brecciated and fractured state, with cavities producing higher porosity; and the more iron-poor composition of ferromagnesian minerals with lower densities.

The magnetic susceptibility, intensity of NRM and Q-ratio data of the sedimentary rocks, as also other parameters in Table 3, show the sedimentary rocks to belong mainly to the paramagnetic population, and the higher susceptibilities are in most cases due to the presence of pyrrhotite. This points to an overall reducing environment, as also seen in the common occurrence of graphite in these rocks. The occurrence of both pyrite- and pyrrhotite-dominated sedimentary rocks suggests an irregular conversion of pyrite to pyrrhotite in the presence of graphite, as proposed by Peltonen (1995) for the Vammala area, located in the continuation of the MB area to the west. The SG1 samples are considered to be of direct arc origin and they are closely associated with volcanics. The occurrence of magnetite in some samples may be due to direct derivation from a magnetite-bearing source, but a metamorphic origin cannot be excluded. The high-grade migmatites from the MC contain metamorphic magnetite. Lahtinen (1996) has suggested that, during the metamorphism, there has been a loss of graphite, some trace elements and even sulphur producing more oxidizing conditions which were favourable for magnetite crystallization.

The volcanic rocks in the MB are either paramagnetic or contain pyrrhotite. The tholeiitic volcanics (VG2–VG3) in the HSB (Häme group) show both magnetite- and pyrrhotite-dominated properties (Table 3). Samples with inferred magnetite (low Q-ratio) are often the most differentiated and enriched or else contaminated variants, which along with the common pyroclastic nature indicates fluid enrichment. A similar situation exists in the calc-alkaline magnetite-bearing rocks (VG5–VG6) and thus it seems that the volatile content of the magma or increase in the amount of volatiles during differentiation, change in the chemical composition (e.g. contamination) or new external water supply (e.g. ground water) can induce magnetite crystallization. The situation is complex, however, since the amount of magnetite that forms can vary within the same flow or cooling unit, with the most fluid-enriched part containing more magnetite. On the other hand, continuous fluid flow and alteration may break down the magnetite to martite or hematite, as seen in the low and high susceptibility rock pairs (p. 28). Subduction-related groups VG3, VG5 and VG6 (Lahtinen 1996) show a high proportion of samples with abundant magnetite, which is in accordance with the water-rich nature of subduction-related magmas in general, producing a calc-alkaline crystallization trend and magnetite precipitation (see discussion in Lahtinen 1996).

The two mafic plutonics from the NTSB with highest content of magnetite are strongly differentiated high-Ti tholeiitic rocks with abundant K, Ba, Th, La, P and Zr. The occurrence of magnetite can be attributed to high water content and oxidizing conditions in highly evolved mafic magma and/or to the interaction of mafic with felsic magma producing comparable conditions. Similar features are noticed in some other magnetite-bearing mafic plutonics in the study area. The occurrence of pyrrhotite is responsible for the elevated susceptibilities in some mafic plutonics in the MB and HSB.

The higher susceptibilities in granitoids are mainly due to magnetite±hematite since there are no samples with predicted dominance of pyrrhotite. Syn-tectonic granitoids (GG1–GG4) belong mainly to the paramagnetic population and magnetite occurs mainly in granitoids of comingled and hybrid nature. This suggests an interaction with mafic magmas as the probable cause of magnetite crystalliza-

tion in favourable conditions. Magnetite may also be due to totally resorbed small mafic magma blobs in the granitoids.

A large proportion of samples in groups GG5 and GG6 (excluding HSB subgroup) bear ferrimagnetic susceptibilities (92% and 87%, respectively). The proportion of samples belonging to the dominantly ferrimagnetic population is also large (77% and 69%, respectively). Although the magnetic susceptibilities are not very high, there is a prevalent occurrence of magnetite±hematite. These are late- to post-tectonic (1.88–1.86 Ga) granitoids of tholeiitic affinity proposed to have originated in the melting of crustal rocks (GG5) and WPB-affinity mafic underplate±crustal rocks (GG6) (Lahtinen 1996). The iron-rich nature of the parent magmas is the inferred cause of the general crystallization of magnetite (±hematite) in these rocks. Although the primary nature of the hematite in these samples cannot be ruled out, the abundant occurrence of martite and hematite in some granites (e.g. the GG6 granite of pair 6 in Table 2) suggests that it has more likely originated in connection with percolating late magmatic fluids, groundwater intruding during emplacement or influx of younger fluids. The S-type microcline granites (GG7) from both the MB and MC, and the GG8 samples from the MB and HSB all belong to the paramagnetic population.

The MC exhibits the highest regional magnetization in the study area, especially if we exclude the microcline granite dominated northern part of the MC. The occurrence of magnetite-bearing migmatites explains, at least in part, the irregularly shaped shallow anomalies. Some strongly foliated granitoids also contain magnetite, but it is not known whether they are of primary or metamorphic origin. The high total contents of La, P and Sr in regional till geochemical maps in areas characterized by aeromagnetic highs could indicate a high proportion of WP-affinity rocks in these areas. The high magnetic susceptibility of the WP-affinity pluton supports this. The low areal Q-ratio in the MC correlates well with the predominance of magnetite-bearing samples in the ferrimagnetic population, showing that magnetite is the main cause of the magnetic anomalies.

Although the above-considered features explain many of the shallow magnetic highs, the occurrence of a deeply seated magnetic source is required to explain the strong areal high. One obvious candidate is mafic rocks, which would also explain the hidden mass in the MC. The large volumes of felsic S-type granites, on the other hand, argue for the presence of deep-seated restitic rocks. Migmatization is normally confined to about 4–5 kbar in southern Finland (Kilpeläinen et al. 1994, Väisänen et al. 1994 and references therein) and a similar or lower emplacement depth is indicated for the MC granites. The proposed melting depth is about 6–7 kbar (Lahtinen 1996), so that restite rocks would be at 3 to 10 km depth relative to the present erosion level. Since metamorphic magnetite occurs in the MC migmatites, magnetite could also occur in the restite, and thus the restite could provide a partial or even an alternative explanation of the deep magnetic and gravity anomalies.

Judging from the magnetic and gravity anomalies the HSB is a moderately thick formation, possibly with some deep-seated sources. The irregularly shaped, strong and shallow magnetic anomalies are mainly due to VG3 and VG5 volcanics, but some of them are due to mafic plutonics. The magnetic anomalies are mainly attributable to magnetite-bearing rocks, but pyrrhotite-bearing rocks make a significant contribution. This is also seen in the higher areal Q-ratio in the HSB than the MC.

The negative regional magnetic anomaly in the MB is probably due to the thick pile of mainly paramagnetic sedimentary rocks and granitoids. The gravity data imply local hidden masses probably due to mafic bodies. The total absence of magnetite in the MB, regard-

less of rock type, points to an overall reducing environment. The igneous rocks very often show a sediment-assimilated nature, as seen also in the occurrence of graphite in some samples. Although the occurrence of magnetite in the MB rocks cannot be ruled out, the data of this study indicate the predominance of pyrrhotite in producing the local magnetic anomalies. In other areas, WP-affinity and hybrid plutonics are the most common magnetite-bearing plutonic rocks. While these types of rocks are not uncommon in the MB, no magnetite has been found in them. Thus, the lack of magnetite is most probably due to the sedimentary pile with abundant occurrence of graphite and sulphides producing a reducing environment that inhibited magnetite crystallization. Although we favour this explanation of the absence of magnetite, we note as well the possibility of its breakdown during metamorphic reactions as proposed by Ruotoistenmäki (1992). The complexity of the situation is seen in the Vammala area where secondary magnetite has been found in some Ni-bearing mafic plutonic rocks (Peltonen 1995)

The TSB can be divided into two parts, of which the southern part, composed mainly of sedimentary rocks and paramagnetic granitoids, is similar to the MB. The northern part is characterized by an abundant occurrence of volcanics, of which the VG5 volcanics and the Upper Volcanite at Ylöjärvi (not sampled in this study) are mainly responsible for the strong anomalies, but also VG6 and VG7 show magnetic features.

The strong and shallow magnetic anomalies of the NTSB are mainly concentrated in the HiSB, where all the volcanic samples and two of four sedimentary samples show the occurrence of magnetite. The irregularly shaped magnetic anomalies are probably due to these supracrustal rocks. The shallow magnetic anomalies in other parts of the NTSB might be due to the concentrations of hybrid comingled rocks and evolved mafic plutonics. The GG5 and GG6 granitoids show general magnetic affinity, but their magnetization is normally rather low. As they are aerially widespread, however, they could, along with the magnetic hybrid variants of other granitoids and evolved mafic plutonics, account in some degree for the strong regional magnetic high observed in the NTSB. A strong, deep and variable magnetic source of felsic nature is nevertheless also required. The preliminary data suggest that the GG5 and GG6 granitoids contain abundant martite±hematite and if this were due to weathering, concentrating near the present erosion level, the occurrence of more magnetized samples (fresh magnetite) in the deeper part of the crust would be indicated (see below).

The source of the elevated intensity of NRM (>50–60 mA/m) in some paramagnetic samples remains problematic. The occurrence of a small amount of ferrimagnetic minerals also in 'paramagnetic' rocks implies, in fact, that true paramagnetic rocks are rare or lacking, and the NRM may be related to these minute crystals of ferrimagnetic material. The equation we propose for the relationship between chemically estimated paramagnetic susceptibility and bulk density seems very promising, allowing the division of density–susceptibility data into paramagnetic ($X \leq X_{pp}$) and ferrimagnetic ($X > X_{pp}$) samples, and into paramagnetic, ($(X-X_{pp}) \leq X_{pp}$) and ferrimagnetic populations ($(X-X_{pp}) > X_{pp}$) (see p. 14). The $X_{pp} = X_{pd} + 4.1 m^3/kg$ (see eq. in p. 28) and includes 95% of the estimated paramagnetic population.

The one major question is the common occurrence of martite and hematite together with magnetite skeletons. Whether this magnetite breakdown, which in most cases decreases the magnetization of the rock, is due to synvolcanic and synplutonic alteration, ground water circulation at the emplacement depth or surface oxidation processes is unclear. If there is considerable influence from processes operating at the emplacement depth of intrusive rocks or, later, at the present erosion

level, the average magnetizations will be underestimated and the extrapolation to deeper levels, at least in part, will be invalid. The proposed overall reducing environment in the MB would inhibit the crystallization of magnetite in rocks which in other areas would show a significant amount of samples in ferrimagnetic population. If this is true, the ferrimagnetic properties of rocks cannot be used to classify rocks intruding in reducing environment.

The results presented above can now be integrated with the evolutionary model for the study area proposed by Lahtinen (1996; see also Lahtinen 1994). Basement-related sediments (SG3–SG7) are related to the pre-1.91 Ga rifting stage and/or to the 1.91–1.90 Ga collision in the northeast against the Archaean craton. Magnetite is lacking in these sediments, and evidently was lacking even at deposition, since absence of magnetite also characterizes the rocks adjacent to the magnetite-bearing volcanics in the TSB. Subduction-related calc-alkaline volcanic rocks in both the TSB (1.91–1.89 Ga) and HSB (>1.89 Ga) show abundant magnetite, which at least partly is due to the volatile-rich nature (subduction component) of the parent magmas. The tholeiitic linear rift-related VG3 (about 1.89 Ga) volcanics and the Upper Volcanite at Ylöjärvi (1.89 Ga, Kähkönen 1989) show the occurrence of both subduction component and abundant magnetite.

During the late stages of collision, syn-tectonic calc-alkaline granitoids (GG2–GG4 excluding GG3 Nokia-type, 1.89–1.88 Ga) intruded. These are not co-genetic with volcanics and are characterized by mixed origin (Lahtinen 1996). These are also mainly paramagnetic rocks, while magnetic variants are normally confined to rocks that show comingling and hybridization with mainly tholeiitic mafic magmas (extra input of Fe). One way to explain the difference between calc-alkaline volcanics (abundant magnetite) and intrusive rocks (lacking magnetite) is that magnetite has been a precipitating phase in magmas forming calc-alkaline volcanics (lowering FeO/MgO ratio), and has been confined in the source residue during the melting of the crustal source forming the crustal component of these syn-tectonic granitoids (Lahtinen 1996).

Vapour-phase-present conditions prevailed during the syn-tectonic stage (Lahtinen 1996) and probably explain the partial conversion of sedimentary pyrites to pyrrhotite as proposed by Peltonen (1995). The continuous heating during magmatic underplating and vapour-phase-present melting reactions dried the crust, and during the late- to post-collisional stage (1.88–1.86 Ga) vapour-phase-absent melting dominated (Lahtinen 1996). Late- to post-tectonic granites (GG5–GG6) in the NTSB are characterized by ferrimagnetic minerals (magnetite+martite), and their high FeO/MgO ratio means that there could not have been a large amount of magnetite in the source residue. The abundances of these ferrimagnetic minerals are low, on the other hand, and these rocks do not generate strong magnetic anomalies.

The intracrustal collision about 1.86–1.84 Ga ago was followed by the intrusion of large amounts of minimum melt granites (1.84–1.81 Ga) in the MC. Their derivation was preceded by fluid loss, probably during the earlier 1.89–1.88 Ga event. These granites are paramagnetic rocks with variable FeO/MgO ratios, which indicate variable FeO/MgO ratios in the source, crystal differentiation, or variable amounts of magnetite in the source residue. The occurrence of metamorphic magnetite in pelitic migmatites indicates that magnetite crystallization in the source residue is possible.

Taken together, the magnetic and gravity data indicate that the MC is a relatively thick formation underlain by hidden mass and a deep magnetic anomaly component probably related to mafic or restite rocks, or both. The NTSB, on the other hand, is a rather shallow formation underlain by low density rocks with

variable magnetization. Possible explanations of the deep magnetic source are the occurrence of magnetite-bearing siliceous restites and the occurrence of less oxidized (containing more magnetite) late- to post-tectonic granites in the middle crust. The MB is considered as a collision zone with maximum shortening (Lahtinen 1996), and this is in good agreement with our interpretation of the magnetic and gravity data, indicating a relatively deep continuation for the MB with larger amounts of mafic rocks locally.

CONCLUSIONS

– The correlation between density and FeO+MnO+MgO is good for the metavolcanic and plutonic rocks but poorer for the metasedimentary rocks due to more complex mineralogy.

– Chemical estimations of the paramagnetic susceptibility together with susceptibility measurements allow a division of the samples into paramagnetic (78%), and ferrimagnetic populations (22%), where 16% may cause anomalies higher than 50 nT and 4% higher than 500 nT for sheet like bodies.

– Chemically estimated ferrimagnetic Q-ratios and sulphur values can be used to classify the ferrimagnetic samples into pyrrhotite- and magnetite-dominated populations.

– The mean Q-value (all samples, paramagnetism neglected) is 2.8 varying from 0.2 to 2.1 for magnetite-dominated, from 2.1 to 7.7 for mixed and from 15.1 to 16.0 for pyrrhotite-dominated populations.

- Pure paramagnetic samples are rare or absent in our sample population; virtually all paramagnetic samples show a small ferrimagnetic component (about $2 \cdot 10^{-8}$ m^3/kg) explaining the occurrence of NRM and thus the term paramagnetic population for lower susceptibility population may be misleading.

– Subduction-related volcanics often contain magnetite±martite±hematite, but the correlation tends to be more with the brecciated and pyroclastic nature of these rocks.

– The magnetite-bearing mafic plutonic rocks often are highly evolved or contaminated variants.

– The syn-tectonic (1.89–1.88 Ga) granitoids are mainly paramagnetic. Most magnetite-bearing variants are rocks that have interacted with tholeiitic mafic magma.

– Late- to post-tectonic granites (1.88–1.86 Ga) in the northern part often contain small amounts of magnetite±martite.

– The magnetization in the Microcline-granite Complex (MC), Tampere Schist Belt (TSB) and North of Tampere Schist Belt (NTSB) is due to magnetite. A reducing environment is indicated for the Mica gneiss-migmatite Belt (MB) and the presence only of pyrrhotite among ferrimagnetic minerals. Evidently both magnetite and pyrrhotite are present in the Hämeenlinna Schist Belt (HSB).

– The high regional anomaly of the magnetic field in the MC (+ 80 nT) and NTSB (+100 nT) relative to the MB (regional anomaly -250 nT) indicates that the MB is a relatively deep formation. The occurrence of a deep magnetic source is indicated for the MC and NTSB, and the MC is also underlain by hidden excess mass (mafic rocks and/or restites).

– Although the correlation between petrophysical and geochemical characteristics of rocks is not always straightforward the results of this study demonstrate the utility of petrophysical–geochemical comparisons in studying the origin of rocks and the processes affecting them, and in evaluating surface and deep potential field anomalies.

ACKNOWLEDGEMENTS

This work was a joint study of the Rock Geochemistry Research Project and the Crustal Model Program, both being carried out at the GSF. The other members of these two projects are warmly thanked for their efforts and contributions. Special thanks go to S. Elo for the gravity data, to Maija Kurimo for magnetic low-altitude data, to L. Kivekäs for taking responsibility for the petrophysical measurements and to T. Laine for the paramagnetic measurements. This paper benefitted from a review by I. Kukkonen and from comments by T. Ruotoistenmäki and H. Säävuori. R. Salminen is thanked for editing the manuscript and K. Ahonen for revising the language.

REFERENCES

Deer, W.A., Howie, R.A. & Zussman, J., 1962a. Rock-Forming minerals Vol. 1 Ortho- and Ring Silicates. London: Longmans, Green and Co Ltd. 333 p.

Deer, W.A., Howie, R.A. & Zussman, J., 1962b. Rock-Forming minerals Vol. 3 Sheet Silicates. London: Longmans, Green and Co Ltd. 270 p.

Deer, W.A., Howie, R.A. & Zussman, J., 1963a. Rock-Forming minerals Vol. 2 Chain Silicates. London: Longmans, Green and Co Ltd. 379 p.

Deer, W.A., Howie, R.A. & Zussman, J., 1963b. Rock-Forming minerals Vol. 4 Framework Silicates. London: Longmans, Green and Co Ltd. 435 p.

Elo, S., 1992. Gravity anomaly maps. In: Koljonen, T. (ed.) Geochemical atlas of Finland, part 2. Till. Geological Survey of Finland, 70–75.

Hakkarainen, G., 1994. Geology and geochemistry of the Hämeenlinna–Somero volcanic belt, southwestern Finland: a Paleoproterozoic island arc. In: Nironen, M. & Kähkönen, Y. (eds.) Geochemistry of Proterozoic supracrustal rocks in Finland. Geological Survey of Finland, Special Paper 19, 85–100.

Henkel, H., 1976. Studies of density and magnetic properties of rocks from northern Sweden. Pageoph 114, 235–249.

Hrouda, F., 1994. A technique for the measurement of thermal changes of magnetic susceptibility of weakly magnetic rocks by the CS–2 apparatus and KLY–2 Kappabridge. Geophysical J. Int. 118, 604–612.

Kähkönen, Y., 1989. Geochemistry and petrology of the metavolcanic rocks of the early Proterozoic Tampere Schist Belt, southern Finland. Geological Survey of Finland, Bulletin 345. 104 p.

Kilpeläinen, T., Korikovsky, S., Korsman, K. & Nironen, M., 1994. Tectono-metamorphic evolution in the Tampere–Vammala area. In: Pajunen, M. (ed.) High temperature-low pressure metamorphism and deep crustal structures. Meeting of IGCP project 304 'Deep Crustal Processes' in Finland, September 16–20, 1994. Geological Survey of Finland, Guide 36, 27–34.

Kivekäs, L., 1993. Density and porosity measurements of the Petrophysical laboratory of the geological Survey of Finland. In: Autio, S. (ed.) Current Research 1991–1992. Geological Survey of Finland, Special Paper 18, 119–127.

Korhonen, J.V., 1992. Magnetic properties of the bedrock. In: Alalammi, P. (Ed.) Atlas of Finland 123–126, Geology, Appendix, 15.

Korhonen, J.V., Säävuori, H., Wennerström, M., Kivekäs, L., Hongisto, H. & Lähde, S., 1993. One hundred seventy eight thousand petrophysical parameter determinations from the regional petrophysical programme. In: Autio, S. (ed.) Current Research 1991–1992. Geological Survey of Finland, Special Paper 18, 137–141.

Lahtinen, R., 1994. Crustal evolution of the Svecofennian and Karelian domains during 2.1–1.79 Ga, with special emphasis on the geochemistry and origin of 1.93–1.91 Ga gneissic tonalites and associated supracrustal rocks in the Rautalampi area, central Finland. Geological Survey of Finland, Bulletin 378, 128 p.

Lahtinen, R., 1996. Geochemistry of Palaeproterozoic supracrustal and plutonic rocks in the Tampere–Hämeenlinna area, southern Finland. Geological Survey of Finland, Bulletin 389. 113 p.

Nesbitt, H.W. & Young G.M., 1982. Early Proterozoic climates and plate motions inferred from major element chemistry of lutites. Nature 299, 715–717.

Peltonen, P., 1995. Magma–coutry rock interaction and the genesis of Ni–Cu deposits in the Vammala Nickel Belt, SW Finland. Mineralogy and Petrology 52, 1–24.

Peltoniemi, M., 1995. Electrical conductivity of rock and soil types. In: Alalammi, P. (ed.) Atlas

of Finland 123–126, Geology, Appendix, 15–16.

Pennanen, M., 1991. Selvitys malmimikroskooppisista ja petrografisista tutkimuksista petrofysiikan ohjelmaan vv. 1990–1991. Geological Survey of Finland, unpublished report, Q11/91/1. 16 p.

Puranen, M. & Puranen, R., 1977. Apparatus for the measurement of magnetic susceptibility and its anisotropy. Geological Survey of Finland, Report of Investigation 28. 46 p.

Puranen, R.,1989. Susceptibilities, iron and magnetite content of Precambrian rocks in Finland. Geological Survey of Finland, Report of Investigation 90. 45 p.

Puranen,R., Elo, S. & Airo, M-L., 1978. Geological and areal variation of rock densities, and their relation to some gravity anomalies in Finland. In: Saxov, S. (ed.) Proceedings of the Symposium on the Role of Density. GeoSkrifter 10: Aarhus University, 123–164.

Puranen, R. & Sulkanen, K., 1985. Technical description of microcomputer-controlled petrophysical laboratory. Geological Survey of Finland, unpublished report, Q15/27/85/1. 252 p.

Ruotoistenmäki, T., 1992. Tampereen liuskevyöhykkeen pohjoisreunan ja Keski-Suomen graniitin eteläreunan petrofysiikasta. In: Papunen, H. (ed.) Global Geoscience Transect, Meeting in Turku 14–15.4.1992. University of Turku Publications 31, 52–54.

Sandström, H., 1996. The analytical methods and precision of the element determinations used in the regional bedrock geochemistry in the Tampere–Hämeenlinna area, southern Finland. Geological Survey of Finland, Bulletin 393. 25 p.

Simonen, A., 1980. Prequaternary rocks of Finland. 1:1 000 000. Espoo: Geological Survey of Finland.

SPSS Inc., 1988. SPSS–X Users's guide, 3rd edition, SPSS Inc. Chicago, Ill, USA. 1072 p.

Vaasjoki, M., 1995. Rengon Rouvinmäen Kvartsimontsodioriitti: uusi posttektoninen granitoidi. Summary: The Rouvinmäki quartz monzodiorite at Renko: a new posttectonic granitoid. Geologi 47 (6), 79–81.

Väisänen, M., Hölttä, P., Rastas, J., Korja, A. & Heikkinen, P., 1994. Deformation, metamorphism and the deep structure of the crust in the Turku area, southwestern Finland. In: Pajunen, M. (ed.) High temperature-low pressure metamorphism and deep crustal structures. Meeting of IGCP project 304 'Deep Crustal Processes' in Finland, September 16–20, 1994. Geological Survey of Finland, Guide 36, 35–41.

Vernon, R. H., 1961. Magnetic susceptibility as a measure of total iron plus manganese in some ferromagnesia silicate minerals. The American Mineralogist 46, 1141–1153.

Tätä julkaisua myy

GEOLOGIAN
TUTKIMUSKESKUS (GTK)
Julkaisumyynti
PL 96
02151 Espoo
☎ 0205 50 11
Telekopio: 0205 50 12

GTK, Väli-Suomen
aluetoimisto
Kirjasto
PL 1237
70211 Kuopio
☎ 0205 50 11
Telekopio: 0205 50 13

GTK, Pohjois-Suomen
aluetoimisto
Kirjasto
PL 77
96101 Rovaniemi
☎ 0205 50 11
Telekopio: 0205 50 14

Denna publikation säljes av

GEOLOGISKA
FORSKNINGSCENTRALEN (GFC)
Publikationsförsäljning
PB 96
02151 Esbo
☎ 0205 50 11
Telefax: 0205 50 12

GFC, Distriktsbyrån för
Mellersta Finland
Biblioteket
PB 1237
70211 Kuopio
☎ 0205 50 11
Telefax: 0205 50 13

GFC, Distriktsbyrån för
Norra Finland
Biblioteket
PB 77
96101 Rovaniemi
☎ 0205 50 11
Telefax: 0205 50 14

This publication can be obtained
from
GEOLOGICAL SURVEY
OF FINLAND (GSF)
Publication sales
P.O. Box 96
FIN-02151 Espoo, Finland
☎ +358 205 50 11
Telefax: +358 205 50 12

GSF, Regional office for
Mid-Finland
Library
P.O. Box 1237
FIN-70211 Kuopio, Finland
☎ +358 205 50 11
Telefax: +358 205 50 13

GSF, Regional office for
Northern Finland
Library
P.O. Box 77
FIN-96101 Rovaniemi, Finland
☎ +358 205 50 11
Telefax: +358 205 50 14

ISBN 951-690-668-0
ISSN 0367-522X

9 789516 906686

E-mail: info@gsf.fi
WWW-address: http://www.gsf.fi